

The copyright of this thesis vests in the author. No quotation from it or information derived from it is to be published without full acknowledgement of the source. The thesis is to be used for private study or non-commercial research purposes only.

Published by the University of Cape Town (UCT) in terms of the non-exclusive license granted to UCT by the author.

**THE STUDY OF AN
ADAPTIVE BIT RATE MODEM
FOR
METEOR SCATTER COMMUNICATIONS**

GRAHAM JOHN MEYEROWITZ


A thesis submitted to the faculty of Engineering, University of Cape Town, in partial fulfilment of the requirements for the degree of Master of Science in Engineering.

CAPE TOWN 1990

The University of Cape Town has been given the right to reproduce this thesis in whole or in part. Copyright is held by the author.

DECLARATION

I declare that this thesis is my own, unaided work. It is being submitted for the Degree of Master of Science in Engineering in the University of Cape Town. It has not been submitted before for any degree or examination in any other University.

-----

(Signature of candidate)

13th day of September 1990

To my parents, Lollie and Jackie Meyerowitz.

ACKNOWLEDGEMENTS

I would like to express my appreciation to:

Dr. R. Braun, my supervisor for his invaluable advice and assistance throughout the course of my work.

Mr. P. Handley, for his support, and original motivation, without whom this project could not have been undertaken.

Mr. S. Schrire, for his excellent technical advice.

Mrs. J. Fold, for her administrative help.

Financial assistance from SALBU, PTY, LTD.

Table of Contents

ABSTRACT	i
ACKNOWLEDGEMENTS	iii
CONTENTS	iv
TABLE OF FIGURES	vii
TABLE OF TABLES	ix
C H A P T E R 1 INTRODUCTION	1
1.1 BACKGROUND	1
1.2 HISTORY	2
1.3 SPECIFICATIONS	4
1.4 REFERENCES	7
C H A P T E R 2 THE CHANNEL	9
2.1 CHANNEL CHARACTERISTICS	10
2.1.1 CHANNEL GAIN	11
2.1.2 DOPPLER SPREAD	12
2.1.3 MULTIPATH SPREAD	12
2.1.4 CHANNEL AVAILABILITY	14
2.1.5 NOISE	16
2.1.6 SUMMARY OF CHANNEL CHARACTERISTICS	17
2.2 METEOR SCATTER CHANNEL CAPACITY	19
2.2.1 CHANNEL THROUGHPUT	20
2.2.2 CHANNEL UTILISATION	20
2.3 THEORETICAL ADAPTIVE MODEM OPERATION	20
2.4 ANALYTICAL COMPARISON OF THREE TYPES OF SYSTEMS [1.8] ..	26
2.5 PRACTICAL OPERATIONAL LIMITS	29
2.6 CONCLUSION	32
2.7 REFERENCES	33
C H A P T E R 3 MODULATION TECHNIQUE	35
3.1 INTRODUCTION	35
3.2 HISTORY	37
3.3 BASEBAND NRZ DATA	38
3.3.1 SPECTRAL DENSITY OF NRZ DATA	39
3.4 BINARY PHASE SHIFT KEYING	41
3.5 DIFFERENTIALLY ENCODED BINARY PHASE SHIFT KEYING	45
3.6 SPECTRUM OF BPSK SYSTEMS	46
3.7 OPTIMUM RECEIVER FOR BINARY DIGITAL MODULATION SYSTEMS	47
3.7.1 PERFORMANCE OF THE OPTIMAL RECEIVER	52
3.7.2 PERFORMANCE OF A SUB OPTIMAL RECEIVER	53
3.7.3 THE EFFECT OF DIFFERENTIAL ENCODING [3.1]	58
3.8 ALTERNATIVE MODULATION SCHEMES	59
3.8.1 QPSK, QQPSK	60
3.8.2 ERROR PERFORMANCE OF QPSK (OPTIMAL RECEIVER) [3.1]	62
3.9 SUMMARY OF MODULATION TECHNIQUES	66
3.10 RATE CHANGE SIGNALLING	67
3.10.1 EXPLICIT SIGNALLING USING the DATA CHANNEL	67
3.10.2 EXPLICIT SIGNALLING USING an AUXILIARY CHANNEL ...	68
3.10.2.1 QPSK WITH TWO INDEPENDENT CHANNELS	70
3.10.2.2 BPSK OR QPSK WITH AN ADDED TONE	71
3.10.2.2.1 Phase Shift Key Modulate (PSK)	80
3.10.2.2.2 Amplitude Shift Key modulate (ASK)	83
3.11 CONCLUSION	84
3.12 REFERENCES	86

C H A P T E R 4	SYSTEM DESIGN AND IMPLEMENTATION	87
4.1	INTRODUCTION	87
4.2	MODULATOR	87
4.2.1	CRYSTAL OSCILLATORS	88
4.2.2	(A) DATA SOURCE	89
4.2.3	(B) DIFFERENTIAL ENCODER	92
4.2.4	(C) VARIABLE FREQUENCY CLOCK GENERATOR	93
4.2.5	(D) VARIABLE FREQUENCY TONE GENERATOR	95
4.2.6	BIT RATE CONTROL	96
4.2.7	(E) SUMMER, CARRIER GENERATOR AND ANALOGUE MULTIPLIER	98
4.2.8	MODULATOR SUMMARY	100
4.3	DEMODULATOR	101
4.3.1	(A) COSTAS LOOP CARRIER RECOVERY	106
4.3.1.1	PHASE VARIANCE	109
4.3.1.2	DYNAMIC RESPONSE	111
4.3.1.2.1	LOOP DESIGN	115
4.3.1.2.2	MULTIPLIERS	116
4.3.1.2.2.1	ARM MULTIPLIERS	117
4.3.1.2.2.2	LOOP MULTIPLIER	117
4.3.1.2.3	LOOP FILTER	117
4.3.1.2.4	ARM FILTERS	118
4.3.1.2.5	VOLTAGE CONTROLLED OSCILLATOR	120
4.3.2	(B) BIT SYNCHRONISATION	123
4.3.2.1	BANDPASS FILTERS	125
4.3.2.2	PHASE-LOCK-LOOP	128
4.3.3	(C) RATE CHANGING CIRCUIT	132
4.3.3.1	BANDPASS FILTERS	132
4.3.3.2	COHERENT DETECTOR	135
4.3.4	(D) DATA RECOVERY AND DECODING	138
4.3.5	DEMODULATOR SUMMARY	141
4.4	INTERFACE WITH HOST COMPUTER	143
4.5	CONCLUSION	144
4.6	REFERENCES	145
C H A P T E R 5	TEST AND MEASUREMENT	146
5.1	INTRODUCTION	146
5.2	ADDED WHITE GAUSSIAN NOISE	147
5.2.1	NOISE SOURCE	148
5.2.2	FINITE CREST FACTOR NOISE	149
5.3	BIT ERROR COUNT	150
5.4	EYE DIAGRAMS	151
5.5	CARRIER RECOVERY	154
5.5.1	LOCAL OSCILLATOR JITTER	157
5.6	BIT TIMING RECOVERY	158
5.6.1	LOCAL OSCILLATOR JITTER	158
5.7	ERROR COUNT (P_e) VS S/N	159
5.8	THE ABILITY OF THE DEMODULATOR TO SWITCH BIT RATE	162
5.9	TRANSMITTING A MESSAGE TO INDICATE THE RATE CHANGE	164
5.9.1	PSK TONE MODULATION	164
5.9.2	ASK TONE MODULATION	167
5.10	CONCLUSION	168
5.11	REFERENCES	171

C H A P T E R 6	CONCLUSION	172
6.1	CHAPTER SUMMARY	172
6.1.1	CHAPTER 1	172
6.1.2	CHAPTER 2	172
6.1.3	CHAPTER 3	173
6.1.5	CHAPTER 4	174
6.1.6	CHAPTER 5	175
6.2	DISCUSSION OF RESULTS	177
6.3	RECOMMENDATIONS	178
6.4	CONCLUDING REMARKS	179
APPENDIX A	NOISE EQUIVALENT BANDWIDTH	A-1
APPENDIX B	PHASE LOCKED LOOP THEORY	B-1
1.1	SECOND ORDER LOOP	B-3
1.2	LOOP STABILITY	B-7
1.3	SUMMARY	B-9
APPENDIX C	COSTS LOOP	C-1
1.1	PHASE VARIANCE	C-1
1.2	TRANSIENT RESPONSE	C-4
APPENDIX D	SWITCHED CAPACITOR FILTER DESIGN	D-1
APPENDIX E	PASSIVE BAND-PASS FILTERS	E-1
1.1	CIRCUIT OF SIX FILTERS IN PARALLEL	E-1
APPENDIX F	ACTIVE BAND-PASS FILTERS	F-1
1.1	CIRCUIT OF SIX FILTERS IN PARALLEL	F-1
APPENDIX G	PROBABILITY OF ERROR	G-1
1.1	PROBABILITY OF ERROR	G-1
1.2	TRANSFER FUNCTION OF OPTIMAL RECEIVER	G-5
APPENDIX H	THE COMPLETE CIRCUIT DIAGRAM OF THE MODEM	H-1

Figure 4.19	: Switched capacitor clock generator.	120
Figure 4.20	: VCO used in Costas loop.	121
Figure 4.21	: Local oscillator signals.	122
Figure 4.22	: Bit timing recovery technique.	124
Figure 4.23	: Delay circuit for timing recovery with output. .	125
Figure 4.24	: Passive band pass filter and output spectrum. ..	126
Figure 4.25	: Multi-tone Phase locked loop with signals.	130
Figure 4.26	: Bandpass filter, output signal and spectrum. ...	134
Figure 4.27	: Tone detector circuit with inputs and outputs. .	138
Figure 4.28	: Measurement of data recovery process.	139
Figure 4.29	: Differential Decoder	140
Figure 4.30	: Original and recovered data stream.	140
Figure 4.31	: Photograph of demodulator.	142
Figure 4.32	: Modem showing inputs and outputs.	143
Figure 5.1	: Noise measurements.	148
Figure 5.2	: Noise generator.	149
Figure 5.3	: Bit error counter.	151
Figure 5.4	: Eye diagrams of a received bit stream.	152
Figure 5.5	: Arm voltages of a locked loop.	156
Figure 5.7	: Carrier recovery clock jitter.	158
Figure 5.8	: Phase locked loop clock jitter.	159
Figure 5.9	: Pe vs S/N at fb = 4 kbps.	161
Figure 5.10	: PSK tone demodulation.	164
Figure 5.11	: Bit error rate test on the modulated tone.	166
Figure 5.12	: ASK tone demodulation.	168
Figure A1	: NOISE EQUIVALENT BANDWIDTH	A-1
Figure B1	: BASIC PHASE LOCKED LOOP	B-1
Figure B2	: ACTIVE FILTER	B-3
Figure B3	: TRANSFER FUNCTION OF LOOP FILTER	B-4
Figure B4	: FREQUENCY RESPONSE OF SECOND ORDER LOOP	B-6
Figure B5	: ERROR RESPONSE OF A HIGH GAIN LOOP	B-7
Figure B6	: ROOT LOCUS PLOT OF SYSTEM	B-8
Figure C1	: COSTAS LOOP MODEL	C-1
Figure C2	: TRANSIENT RESPONSE OF COSTAS LOOP	C-5
Figure C3	: COMPLETE LINEAR LOOP APPROXIMATION	C-7
Figure C4	: LINEAR COSTAS LOOP MODEL	C-9
Figure D1	: SWITCHED CAPACITOR CIRCUIT DIAGRAM	D-2
Figure D2	: AMPLITUDE AND PHASE RESPONSE OF FILTERS	D-3
Figure E1	: CIRCUIT DIAGRAM OF PASSIVE BAND PASS FILTERS . .	E-1
Figure E2	: AMPLITUDE AND PHASE RESPONSE OF FILTERS with INPUT AND OUTPUT SPECTRA	E-2
Figure F1	: CIRCUIT DIAGRAM OF ACTIVE BAND PASS FILTERS . . .	F-1
Figure F2	: AMPLITUDE AND PHASE RESPONSE OF FILTERS with OUTPUT SPECTRA	F-2
Figure G1	: MODEM WITH ADDITIVE WHITE GAUSSIAN NOISE	G-1
Figure G2	: CONDITIONAL PROBABILITY DENSITY FUNCTION OF AWGN	G-4
Figure H1	: COMPLETE CIRCUIT DIAGRAM OF MODEM	H-1

C H A P T E R 1

INTRODUCTION

The use of Meteor Scatter Communication Systems for transmitting telemetric and other data across the country is proving to be very popular in South Africa. Current systems operate at constant bit rates of 4 k bit/sec and are limited to average throughputs of 50 bit/sec. A modem is required that will maximise this average throughput of data by offering a selection of higher bit rates. The study of an adaptive variable bit rate modem to perform this task is presented here. The final aim of this thesis is to document the design, implementation and testing of an adaptive bit rate modem.

1.1 BACKGROUND

The orbital path that Earth follows around the sun is filled with meteoric debris from space. These meteors enter the atmosphere and burn up, forming long columns of ionised particles approximately 80-120 kilometres above the Earth's surface. Although they diffuse within a few seconds, the scattered ionised particles reflect radio signals and are of sufficient duration to support radio communication over distances up to 2000 Km, hence the name Meteor Scatter Communication (MSC). These columns, or trails, of ionised particles can be up to 200 km in length [1.1]. The particles dissipate under their own velocities and by upper atmospheric winds. The largest trails can only support communications for up to 3 seconds giving rise to another common name, Meteor Burst Communication (MBC).

The frequency range of meteor-burst radio propagation is 30-100 Mhz, the lower limit being determined by the desire to avoid reflections via the ionospheric scatter mechanism. The upper limit is determined by receiver sensitivity limitations, since reflections at higher frequencies are weaker than those at lower frequencies.

A communication link is set up between two stations when a meteor is oriented in the ionosphere at the critical angle that provides a reflection of waves between the two stations in both directions. The proper orientation is such that the angles of incidence and reflection in the transmitter-meteor-receiver path are equal. An illustration of a link is shown in Fig. 1.1.

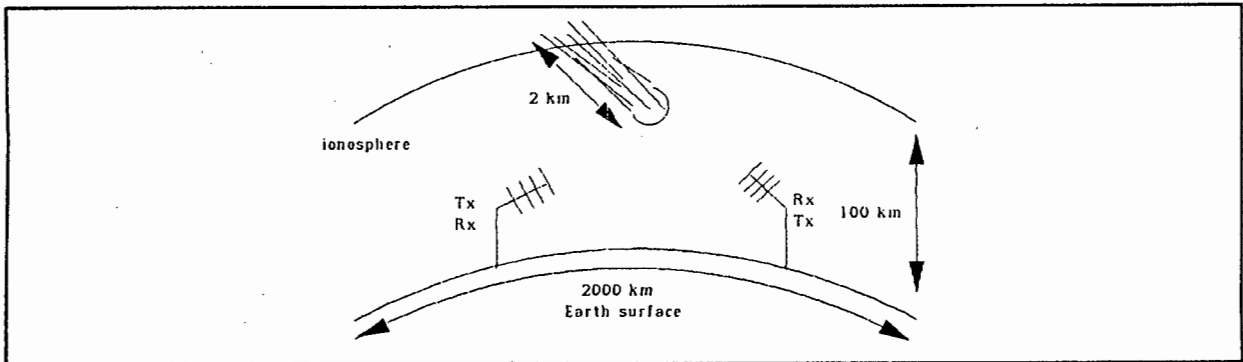


FIGURE 1.1 : Meteor Scatter Communication.

1.2 HISTORY

The possibility of radio wave reflections from meteor trails was first mentioned by Nagaoka in 1927 [1.2] as an explanation for sudden sharp increases in shortwave broadcast reception. In 1931 Pickard [1.3] noticed that these propagation anomalies increased during meteor showers. It was thus established that radio propagation could occur via scattering from inhomogeneities in the upper atmosphere and in particular from meteor scatter. The three modes of propagation become known as Ionoscatter (irregularities in lower ionosphere), Meteorscatter (re-radiation from ionised trails caused by burn up of meteors), Troposcatter (irregularities in troposphere).

In 1935, Skellet [1.4] postulated that the mechanism of reflection was free electrons in the meteor trail. The onset of the second world war put an end to most civilian meteor scatter research.

During 1957 much literature appeared in the Proceedings of the IRE covering meteor scatter theory and techniques. One such article [1.9] discusses the potential of a variable bandwidth system which lays the groundwork for the adaptive, bit rate modem. Progress of these systems was hindered by the magnetic storage equipment that could not operate at the high speeds required.

Also in 1957 experimental evidence proved the use of meteor scatter for facsimile communication. Frequency modulation was used at a bandwidth of 27 kHz [1.10]. In the seventies, interest in meteor scatter was renewed because of the development of microprocessors, enabling inexpensive implementation of sophisticated system control and inexpensive solid-state memories and components.

In 1977 the STC communications system, COMET [1.5], showed the usefulness of a constant bit rate system, which used Automatic Request for Repetition (ARQ) and diversity reception to provide several telegraph channels on a 1000 km path. In the concluding paragraph it was stated that "it is possible to establish several 50-baud communication channels with very high reliability. The only drawback is that time delays of one minute or so can occur due to the intermittent nature of the propagation." The text goes further to predict that "a tenfold increase in signalling rate of 20 000 baud can readily be used," but on the average, "the most practical increases in transmission rate would be one which resulted in a minimum average rate of 2000 baud. This would require burst rates of between 20 to 80 kbit/sec, depending on the other circuit parameters."

Improvements in throughput using an adaptive rate modem became a reality in the eighties, with the ever more reliable and fast solid state devices. In 1987 Weitzen [1.6] concluded that bit rates up to 1 Mbit/sec can be accommodated over meteor trails for a short periods during any one day, only if an adaptive scheme is used.

The interest in Meteor Scatter Communications has been sustained because it is a cheap alternative to satellite communications for beyond-line-of-sight links. The use is however limited to intermittent data communication.

Also in 1987 bit rates of 64 kbit/sec and message lengths of 8000 characters had been achieved using a technique called *dynarate* [1.7]. This implies the ability to dynamically vary the data rate as a function of received signal strength. In this way, maximum bit rates of 500 kbit/sec have been predicted. Another technique to control the operating bit rate that is very microprocessor intensive has been reported [1.8].

The progress from constant bit rate modems to variable bit rate systems has thus been described. It is with these developments in mind that further work is required to achieve maximum throughput of data over the channel in the short link time available by exploiting the concept of an adaptive variable bit rate modem.

1.3 SPECIFICATIONS

The modem is the interface between the computer and the transmitter/receiver unit as shown in Fig. 1.2.

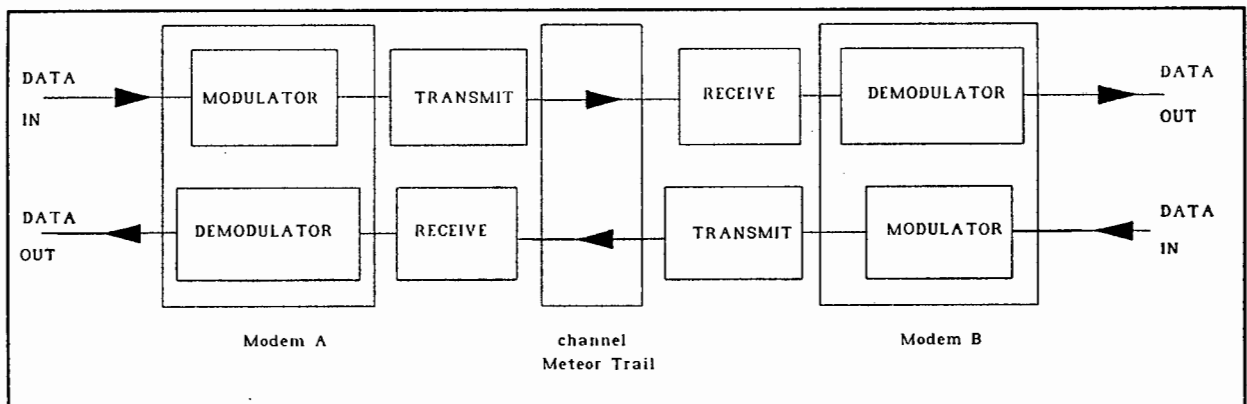


Figure 1.2 : A block diagram of the complete communication system.

The hierarchy of a complete Meteor Burst system consists of many layers of hardware from the controlling computers to the

antennas. The modem is part of the physical layer which also includes, the RF transmitter and the RF receiver. The data link layer consists of a host computer which communicates directly with the modem via an RS-232 link. The figure shows the position of the modem in the complete system. The system is full duplex. Such systems are presently being used at a constant bit rate of 4 kb/sec in South Africa. An adaptive bit rate modem will replace the constant bit rate modem in such a system. The design of an adaptive variable bit rate modem begins with specifications as set out in table 1.1.

The contents of this thesis are outlined as follows. Chapter two is a discussion of the properties of a meteor channel and how the channel affects radio waves. The results of this chapter lay the ground work for the choice of modulation technique. Chapter three presents the various digital modulation techniques that are feasible on a meteor scatter link. The chosen modulation technique, and methods of adaptively varying bit rate. The result of this chapter is the system that will be designed and implemented. Chapter four documents the design and implementation of the modem.

Chapter five includes the tests performed on the actual system and the results obtained by measurement. The conclusion of the thesis is given in chapter six. A short conclusion has been included at the end of each chapter.

Data rate	4 Kbit/sec to more than 100 Kbit/sec
Maximum bit rate step	2:1
Modulation format	Any
Input data	NRZ, synchronous, RS-232
Input Carrier Frequency	700 KHz (Input from power amplifier)
Input data clock	Generated by modem (Input from computer)
Output	Shaped baseband data or 21.4 Mhz modulated carrier (Output to power amplifier).
Carrier synchronisation time	6 m sec maximum.
Bit clock sync. time	6 msec maximum.
Modem synchronisation time	10 msec maximum.
Data rate switching	Seamless, preserving phase continuity.
Output S/N measurement	Not required.
Forward error correction	Not required.
Expected Bit Error Rate (BER)	10^{-2} to 10^{-8} .
TABLE 1.1 : Specifications of the adaptive bit rate modem.	

NOTE :

1. The modulator is to accept commands from a host computer as to which bit rate should be current and exactly when to change bit rate.
2. The demodulator is to change to a new bit rate by way of a signal which is sent by the transmit station just before the bit rate takes place. The bit rate change is to be made without error (seamlessly).

1.4 REFERENCES

- [1.1] Oetting, J. D., **An Analysis of Meteor Burst Communications for Military Applications**, IEEE Trans. on Comms. Vol. COM-28 No. 9 SEPT. 1980.
- [1.2] Nagaoka, H., **Possibility of disturbance of radio transmissions by meteor showers**, Proceedings Imperial Academy of Tokyo, No. 5 , 1929.
- [1.3] Pickard, G. W., **A Note on the Relation of Meteor Showers and Radio reception**, Proceedings of the IRE, vol. 19, No. 7, July 1931.
- [1.4] Skellet, A. M., **The Ionisation Effects of Meteors**, Proceedings IRE, Vol. 23, No. 6, June 1935.
- [1.5] Brown, D. W., **The potential of Meteor-Burst Communications with particular reference to the Comet System**, Communications Division , SHAPE Technical Center, The Hague, Netherlands.
- [1.6] Weitzen, J. A., **The Feasibility of High Speed Digital Communications on the Meteor Scatter Channel**, PhD thesis, University of Wisconsin-Madison, 1983.
- [1.7] Smith, D. K., Donitch, T.J., **Variable Rate Applications In Meteor Burst Communications**, Meteor Communications Corporation, Kent, WA.
- [1.8] Chang, S. S. L., **A Feedback Adaptive Variable Rate Meteor Burst Communication System**, IEEE International Conference On Communications, Philadelphia, P.A., 12-15 June 1988, Digital Technology - Spanning The Universe, Vol. 1 pp 423-429, IEEE , New York, 1988.

- [1.9] Montgomery, G. F., **Intermittent Communication with a Fluctuating Signal**, Proceedings of the IRE Dec. 1957, pp.1678-1684.
- [1.10] Bliss , W. H., Wagner, Jr , R. J. Wickizer, G. S., **Experimental Facsimile Communication Utilising Intermittent Meteor Ionisation** , Proc. IRE , Correspondence pp. 1734 - 1735, Dec.1957.

CHAPTER 2

THE CHANNEL

This chapter deals with the natural channel of the communication system. The natural channel is defined by the environmental limits imposed on a transmitted radio wave between two communicating antennas. This includes the characteristics of the meteor trail pertaining to radio propagation. The discussion of the *non-natural* channel or the *synthetic* channel is done in the following chapter. That includes any filtering done by the modulator and the demodulator.

For the purpose of the discussion of the modem it will be assumed that the transmitter and the receiver, as described by Fig. 1.2, do not modify or interfere with the signal in any way between the output of a modulator and the input to a demodulator over a link. These sub-systems appear transparent to a modulator and a demodulator in one link.

As shown in Fig. 2.1, the natural channel is modelled by a transmittance, $H_c(\omega)$ and Added White Gaussian Noise (AWGN). The synthetic channel is modelled by two transmittances, $H_t(\omega)$ and $H_r(\omega)$ at the transmitter and at the receiver, respectively. The complete channel consists of all three transmittances in cascade.

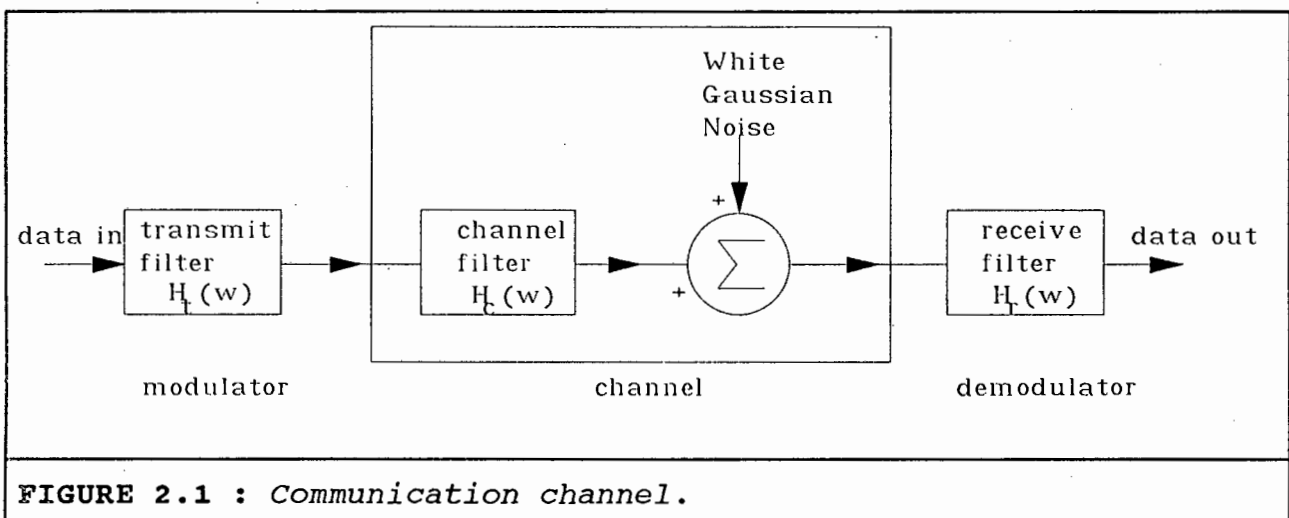


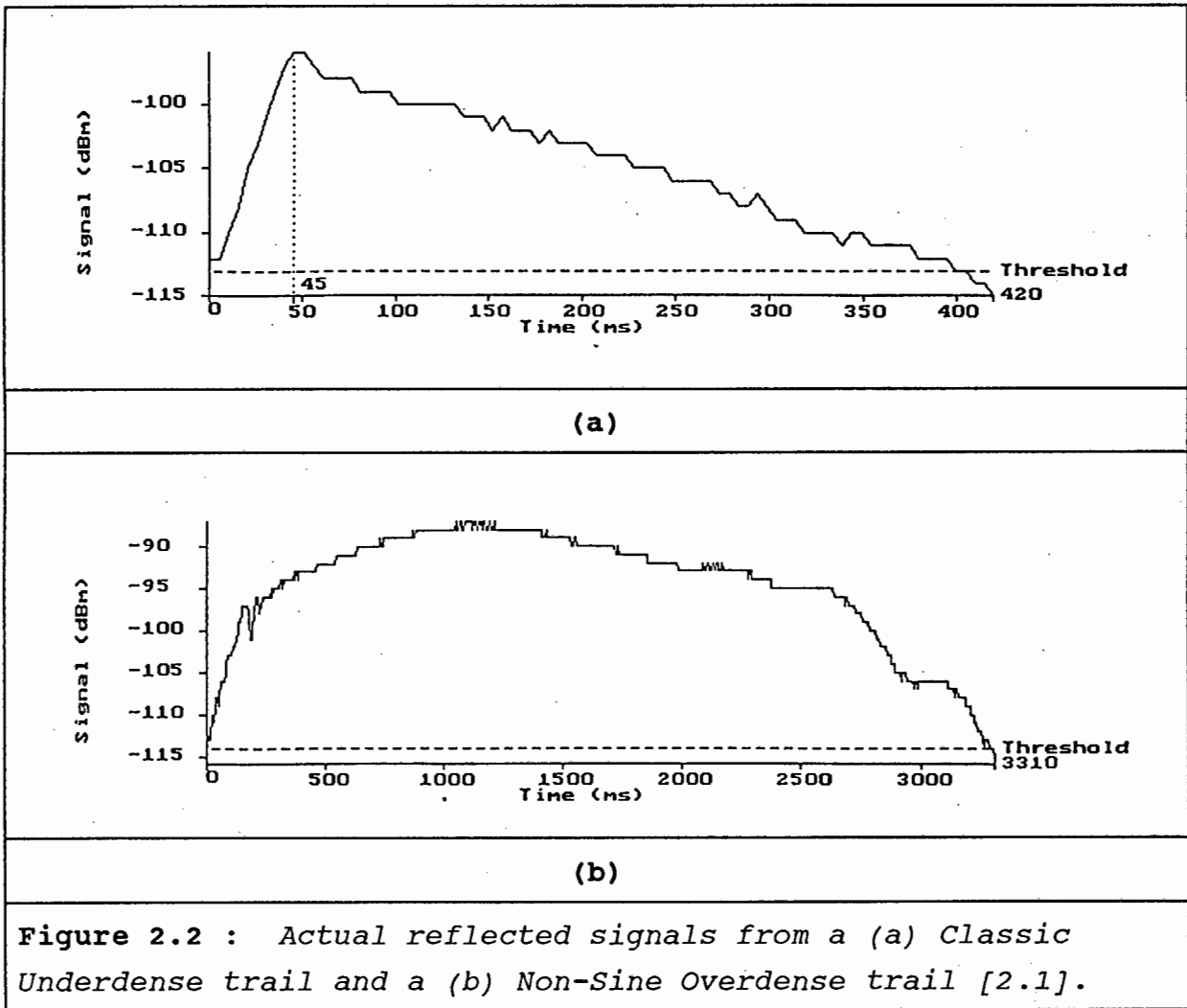
FIGURE 2.1 : *Communication channel.*

2.1 CHANNEL CHARACTERISTICS

The meteor scatter channel has been analysed by other authors and the channel can be completely specified in terms of four parameters: channel gain, Doppler spread, channel availability, and multipath spread [1.6]. This chapter describes these four parameters and shows how they affect radio propagation. A fifth effect on radio propagation is that of noise added to the radio signal, including the modem itself as a contributor.

Meteor trails are broadly characterised as either underdense or overdense, depending on the line density of free electrons in the trail [2.1]. Overdense meteor trails have a high density of free electrons with line densities of 2×10^{14} electrons per meter. This is regarded as a conducting surface. Lower densities are studied as secondary fields where individual electrons perform the reflection. These are under-dense trails which cause scattering by tenuous distributions.

In general, underdense trails are shorter lived but much more numerous than overdense trails. Further classification of trails has been done [2.1] and numerous different classes have been recorded according to the received signal envelope shape. Some examples : Sine Overdense, Classic Underdense and Sinusoidal Overdense. Examples of two such trails are illustrated in Fig. 2.2.



2.1.1 CHANNEL GAIN

The gain of the channel has been described mathematically for both underdense and overdense trails [1.6]. These equations are of no use to the design of the modem since it is preferable to use measurements taken from actual trails. Experimental evidence of the gain can be observed from the received signals from actual trails, with reference to Fig. 2.2. From these two trails and others that have been recorded in the reference [2.1], the following summary has been compiled:

1. Maximum received signal strengths are about -90 dBm.
2. The noise floor of the system defines the lowest signal

strength that can be received, typically -112 dBm. The maximum operating signal-to-noise (S/N) environment is therefore 22 dB.

3. The received gain fluctuates randomly during the existence of a trail, eventually fading to zero dB.

4. The received gain fluctuates from trail to trail with very few trails reflecting signals in the same way.

This confirms the variation in the medium and shows the low signal-to-noise environment that must be expected.

2.1.2 DOPPLER SPREAD

Doppler spread is the frequency spread of the carrier caused by reflections off a moving trail. Since trails are constantly moving the received carrier frequency can shift away from its expected value.

On a meteor scatter link two types of Doppler occur, namely; Body Doppler and Early-fast Doppler. The former type is predominant. The latter is a transient phenomenon observed during the formation of a trail.

Body Doppler has been measured [1.6] for 2200 trails. This data showed that the vast majority of trails have a body Doppler in the range $-2 \text{ Hz} < F_D < 2 \text{ Hz}$. Other work led to the estimate $-1 \text{ Hz} < F_D < 1 \text{ Hz}$ [2.5].

Information about the Doppler Spread therefore indicates that the channel should be able to sustain coherent communications since the magnitude of the shift is well within the limits of typical carrier recovery system lock up times.

2.1.3 MULTIPATH SPREAD

Multipath spread is the time spread of a modulated carrier which defines the phase response of the *natural* channel. The

multipath profile of the channel is generally determined by two distinct phenomena. The first is caused by reflections from the original trail, from a second trail, or from ionospheric effects. The second, less important phenomenon is due to the non-zero radius of a trail [1.6].

In the past, the lack of interest in high speed digital communications on meteor links made detailed studies of the channel multipath profile unnecessary. However, in order to implement high speed modems, it is necessary to establish what the multipath effect is. To do this signals from commercial television stations were received [2.3]. Such signals provide a readily available source of wideband probing signals. Visual multipath measurements were made from TV pictures from Tashkent, USSR received in Pakistan. These experiments showed that 4 Mhz signals were received, for long enough to be visually captured. Wait times for reception of such signals were typically 15 min. The longest burst recorded, lasted 15 sec.

Subsequent experiments done in the USA used an improved method of determining the multipath [1.6]. That is, the vertical equalisation pulses which are transmitted with television programmes have a rigorous specification by the Federal Communications Commission ($2.03 \mu s$ wide spaced every $29 \mu s$). This provided unambiguous multipath information with a resolution of $0.5 \mu s$.

In these experiments, signals were received over a five month period, showing that for most of the trails, spreading was less than $0.6 \mu s$. From these results, it was concluded [1.6] that the coherent bandwidth of the channel and thus the maximum data rate which can be transmitted without Intersymbol Interference is 4 M bit/sec. That is, for short term underdense trails in which the limit is imposed by the non-zero diameter of the trail. The limit reduces to about 2 Mbit/sec for long duration trails in which the maximum rate is imposed by high altitude wind warping.

2.1.4 CHANNEL AVAILABILITY

The availability of the channel is the time available for communications over a twenty four hour period. The occurrence of trails is not continuous and the channel is intermittent, limiting data throughput. Availability depends on:

1. The number of meteors that occur with a high enough electron line density to support communications and the correct orientation with respect to two communicating stations.
2. The length of time that they can sustain communications.

If channel availability is high then the throughput of data will increase. The occurrence of meteors varies daily and seasonally. Meteor showers sometimes occur which increase availability. A statistical analysis of the occurrence of meteor trails is given in sub section 2.3.1. For the sake of a definition, the inherent channel availability during a twenty four hour period is simply calculated as being

$$\text{Availability} = \frac{1}{24 \text{ hours}} \sum_{i=1}^N (\Delta T_u)_i \times 100 \% \quad \text{for } 0 < t < 24 \text{ hours} \quad (2.1)$$

Where : $(\Delta T_u)_i$ = the useable duration of the i^{th} trail.

Availability is the opposite of wait time over any period. Wait time is the average time spent waiting for trails over a twenty four hour period.

Example: to calculate the availability of the link.

When transmitting at a constant bit rate of 4 kbit/sec, a usable trail occurs every one minute, on average, and lasts for one second, on average. This implies an average availability of:

$$A_{\text{ave}} = 1/60 = 0.01666 = 1.67 \%$$

The following is a table representing the number of meteors entering the atmosphere over a twenty four hour period, that have potential for communication [1.6].

Mass (gram)	Radius (cm)	Number of this mass or > per day	Electron line density e/m
10 ³	4.0	10 ²	10 ²⁰
10 ²	2.0	10 ³	10 ¹⁹
10	0.8	10 ⁴	10 ¹⁸
1	0.4	10 ⁵	10 ¹⁷
10 ⁻¹	0.2	10 ⁶	10 ¹⁶
10 ⁻²	0.08	10 ⁷	10 ¹⁵
10 ⁻³	0.04	10 ⁸	10 ¹⁴
10 ⁻⁴	0.02	10 ⁹	10 ¹³
10 ⁻⁵	0.0008	10 ¹⁰	10 ¹²

TABLE 2.1 : *Relative Distribution of meteors as a function of mass [1.6].*

The table is for interest only and will not be used quantitatively. In this discussion it is not necessary to predict the channel availability but it is necessary to define the qualifying terms highlighted above, namely;

1. Which meteors are useable.
2. How long a meteor remains useable after it has come into existence.

It is these limits that will aid the final user in rating the useability of each trail with respect to the modem. With respect to the modem, this time available for transmission must be utilised as efficiently as possible. Synchronisation time at the beginning of a trail must be kept to a minimum. Therefore, the actual time available for data communication

is less than the time of the trail existence because of the practical time limits imposed by circuitry. The utilisation of a trail is considered in section 2.2.2.

2.1.5 NOISE

The noise level at the receiver which defines the minimum signal power that can be received, can consist of any combination of the many noise sources within the frequency range of interest i.e. 30 - 100 Mhz. The two main groups of noise contributors are man-made interference and natural interference [2.2]. A comprehensive list of all noise sources has been given in the reference. One omnipresent and strictly unavoidable form of man-made interference is thermal noise in the receiver components. However, the most prominent noise source is Galactic noise introduced by spurious high-frequency radio waves that penetrate the atmosphere from space.

At the carrier frequency of interest, 50 Mhz, galactic noise does fall off with bandwidth [3.6 chap. 4], however galactic noise is still typically 7 to 16 dB above the thermal noise of receiver. This has been measured from existing systems operating in South Africa. The total noise power at the receiver is assumed to be white and proportional to the bandwidth of the receiver. The total noise power is modelled by a resistor that has a temperature which represents the combination of environmental and receiver noise power:

$$N = kTB \text{ Watts (2.2)}$$

Where:

$k = 1.38 \times 10^{-23}$, Boltzmann's constant, J/°K.

T = noise-source temperature of receiver and the incident galactic noise, °K.

B = bandwidth of received signal, Hz.

The noise threshold at the receiver is set by this power, N . An important explanation of the variables used to indicate signal to noise ratios will now be explained.

Carrier-to-noise ratio will be referred to as S/N or C/N in this text. This is a power ratio of signal power to noise power (Watts / Watts) and is dimensionless. These quantities are measurable in practice using power and root-mean-square (RMS) voltage meters.

The theory of modulation techniques usually refers to E_b/N_o as the signal-to-noise ratio. Where E_b is the received signal energy, having units Watt/Hz, and N_o is noise spectral density, having units Watt/Hz. However, these quantities are difficult to measure in practice. A conversion between S/N and E_b/N_o is given by [3.1, chap. 4] as :

$$\frac{E_b}{N_o} = \frac{C}{N} \left(\frac{B_w}{f_b} \right) \quad dB \quad (2.3)$$

Where: $1/f_b = T$ is the bit period in seconds, B_w is the equivalent noise bandwidth of the receiver, in Hz. For example, the case of the second order Butterworth filter, the values \sqrt{S} and \sqrt{N} are measured by an rms volt-meter at the receiver output, each quantity in the absence of the other. The noise equivalent bandwidth of this filter is , $B_w = 1.1/T$ [appendix A]. Therefore :

$$\frac{E_b}{N_o} = 1.1 \left(\frac{S}{N} \right) \quad dB$$

2.1.6 SUMMARY OF CHANNEL CHARACTERISTICS

Received signal levels rise and fade during the existence of a trail. Each trail has a different maximum and minimum received signal strength and hence the maximum received signal power-to-noise power ratio (S/N) of each trail varies from trail to trail.

The total noise power at the receiver is proportional to the receiver bandwidth and is predominantly caused by the environment. Therefore the S/N received can be increased by decreasing the receiver bandwidth.

Each trail has a different duration. The usable duration of each trail varies from 200 msec. to 3 sec., occasional longer bursts of up to 15 sec. have been recorded. The trails occur intermittently and arrive at any moment.

The Doppler spread has no significant effect on communications.

The multipath effects sets an upper limit on the maximum bit rate. However, the usability of each trail is determined by the received S/N level and not the phase coherence.

The error rate varies up or down proportionally with S/N. In a variable rate system, an attempt is made at maintaining a constant error rate and a constant received S/N level. This is done by adjusting the system bandwidth (bit rate) up or down when the received signal level rises or falls, respectively. This can be explained as follows:

In section [2.1.5] the amount of noise in the system is shown to be proportional to bandwidth. As the received signal power fades it is necessary to reduce the noise power level as well, thereby maintaining a constant S/N. To decrease the noise power at the receiver the bandwidth of the receiver must be reduced. This implies decreasing the bit rate. It can therefore be said that:

1. The maximum bit rate that each trail supports varies from trail to trail.
2. The bit rate that each trail supports varies during its existence. The capacity reaches a peak at some point during the trail and then decays. Some trails have several peaks.

3. High bit rates can only be sustained for short intervals, while the S/N is high.

2.2 METEOR SCATTER CHANNEL CAPACITY

The capacity of the link is therefore determined by the signal-to-noise level received. Useful communication is said to commence once the received signal strength is sufficiently greater than the noise threshold, such that the error rate, $P_e < 10^{-2}$ and the receive bit rate, $B = B_{\min}$ (bit/sec). Where B_{\min} is the lowest (or only) operating bit rate of the modem. Communications ends when the error rate drops below the minimum. For the following discussion of the capacity two definitions are given :

2.2.1 CHANNEL THROUGHPUT

Channel throughput is defined as the total number of bits that can be sent during a trail existence. For a constant bit rate system this can be stated as a bit count

$$TH_{\text{trail}} = T_m \cdot f_b \text{ bits} \quad (2.4)$$

However a more rigorous prediction of the throughput of the channel is done in sub section 2.3.1.

2.2.2 CHANNEL UTILISATION

Channel utilisation is a measure of how well each trail is used. A well utilised channel is one in which the maximum data rate has been transmitted and the throughput has been maximised. The channel utilisation is the actual throughput achieved over a channel divided by the total throughput theoretically achievable over the channel, below a particular error rate, P_e .

$$U = \frac{\text{actual throughput}}{\text{theoretical throughput limit}} \times 100\%$$

The theoretical throughput limit is given in Fig.2.5 of

2.3 THEORETICAL ADAPTIVE MODEM OPERATION

The theoretical operation of an adaptive bit rate modem is now explained. With the aid of an example, the expected results obtained are compared with those of a constant bit rate system.

EXAMPLE

One communicating station, A, probes another station, B. As soon as B receives a signal of relative strength, B transmits back to A acknowledging the link. Let the received signal at B be that of Fig. 2.2 (a). The received signal is at a maximum at -95 dBm and drops off as shown.

Consider the received S/N of the trail shown in 2.2 (a). In this case both the signal and the noise were measured in a 2 Khz bandwidth at the output of the receiver. From the figure, the received S/N level can be determined as

$$\left(\frac{S}{N}\right)_r = P_r, dBm - N_r, dBm \quad dB \quad (2.5)$$

Where P_r is the received signal power and N_r is the noise threshold power. Measurements taken from the figure given in table 2.2. show that the S/N measured in a fixed bandwidth drops with the received signal.

Time (m sec)	50	100	150	200	250	300	350
S (dBm)	-95	-100	-102	-103	-105	-108	-110
N (dBm)	-121	-121	-121	-121	-121	-121	-121
(S/N) dB	26	20	19	18	16	13	11

TABLE 2.2 : Measured received signal-to-noise ratio.

(i) Constant bit rate modem

In a constant bit rate system, the modems do not switch bit rate at all, but maintain the link at one rate until the signals fade and the link terminates. In such a case, it is necessary to select the optimum bit rate for a particular trail. Since trail behaviour is difficult to predict, it becomes impossible to select the best constant bit rate for each trail, that will maximise throughput. There exists a trade off between bit rate and wait time (duty cycle). The use of high bit rates will only be possible with high wait times, the use of low bit rates is possible at shorter wait times.

Consider using the trail at a constant bit rate of 2 kbit/sec, since this trail has been measured in 2 Khz bandwidth. If a Differential Encoded Binary Phase Shift Keyed (DEBPSK) modulation system is used, table 2.2 results in the following probability of error (P_e) for corresponding S/N ratios. A relationship between P_e and S/N for DE-BPSK is available from Fig. 3.1. The origin of this relationship will be explained in the following chapter.

S/N (dB)	P_e
26	$< 10^{-9}$
20	$< 10^{-9}$
19	$< 10^{-9}$
18	$< 10^{-9}$
16	$< 10^{-9}$
13	5×10^{-9}
11	6×10^{-7}

TABLE 2.3 : *Probability of error and received signal-to-noise of a Classic Underdense trail operating at $f_b = 2$ kbit/sec.*

When using a constant bit rate of 2 kbps, this channel has been under utilised since the minimum allowable bit error rate for the modem is $P_e < 10^{-2}$. Thus any received bit error rate below this value is taken to be unnecessarily small. An increase in bit rate can be allowed with a resulting drop in S/N and increase in error rate, as long as the error rate is kept at 10^{-2} .

(ii) Adaptive Variable bit rate modem

In the case of the adaptive bit rate modem, the modems will initially communicate at the slowest bit rate. The receive strength is measured and transmitted back to the respective transmitting station, which then switches to the highest possible rate. This rate is sustained until the received strength drops below, say, -100 dBm and a slower bit rate is required to maintain the P_e . The receiver sends a message to the transmitter to switch down in rate. This changing of bit rates occurs in steps until the receive strength fades below the noise threshold value.

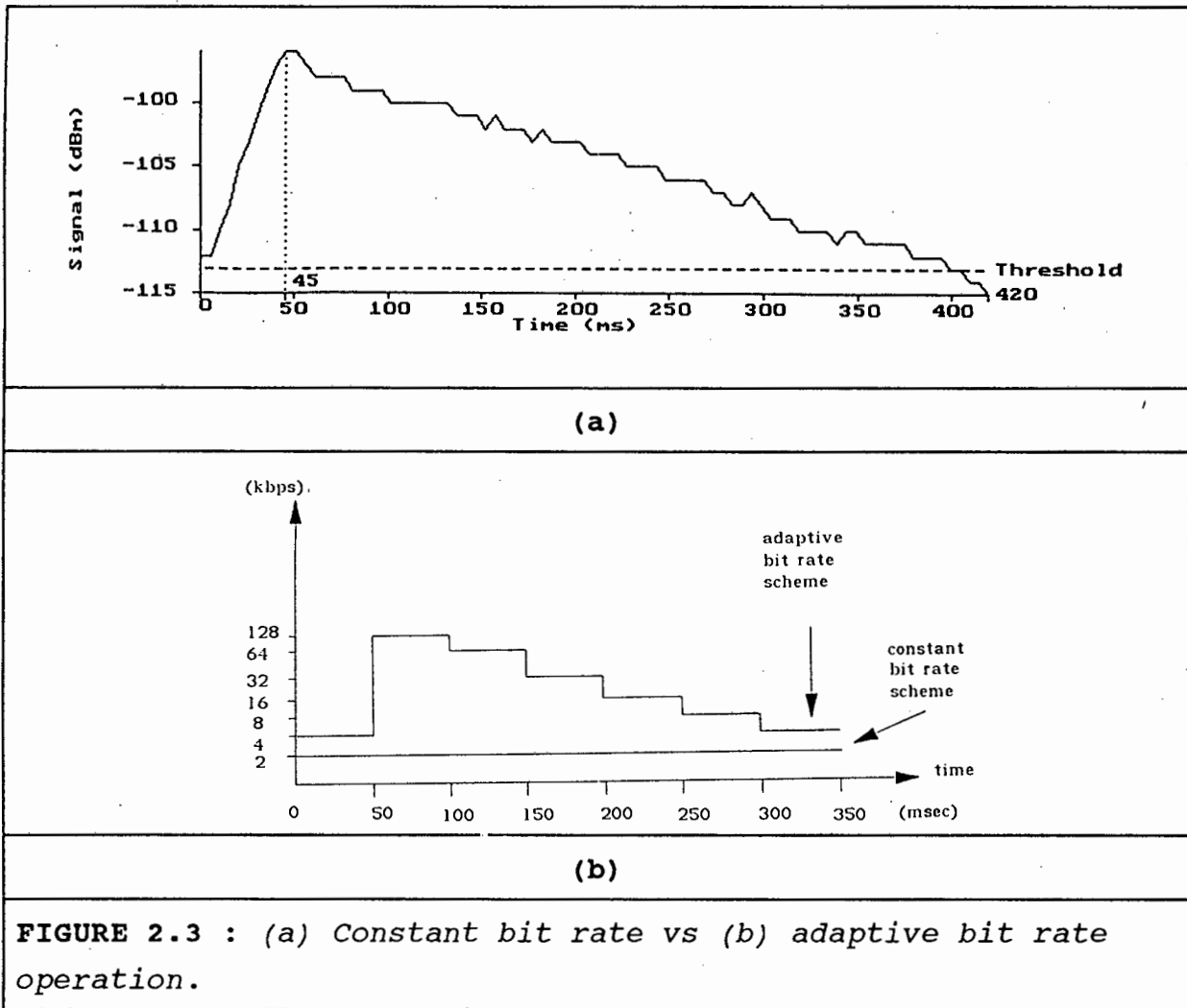
Consider an adaptive bit rate modem operating as explained above. The modem is required to operate from 4 kbit/sec to at least 128 kbit/sec, in multiples of two. Table 2.4 shows the switching rule of the system. The transmitter will switch bit rate according to the absolute S/N measurements in column one. An absolute measurement is one which is taken in a fixed bandwidth (here 2 kHz), irrespective of the current bandwidth of operation. The second column shows the corresponding bit rates. The third column shows the corresponding system bandwidth employing a matched receive filter (see next chapter). This particular S/N vs bit rate relationship has been established for the sake of the example. Notice that the receiver bandwidth decreases as the **absolute** received S/N ratio drops. However, the relative S/N measured at each bandwidth, will be constrained to a small range of values around a chosen set point. An appropriate set point is $P_e = 10^{-3}$ and a S/N = 8 dB.

E_b/N_0^* (dB) (2 kHz bandwidth)	BIT RATE (k bit/sec)	BANDWIDTH (Khz)
> 18	128	128
16 - 18	64	64
13 - 15	32	32
10 - 12	16	16
8 - 10	8	8
< 8	4	4

TABLE 2.4 : Adaptive bit rates versus signal-to-noise ratio.

The two cases are shown in Fig 2.3 (a) and (b) respectively. The constant bit rate operates at one bit rate of 2 kbps only, while the adaptive bit rate modem changes bit rate at the moments in time according to the rule of table 2.4.

* assuming that $E_b/N_0 = S/N$ (the case of Nyquist, matched filters) [3.1]



The increase in throughput can be calculated as follows:

Constant bit rate of 2 kbit/sec

Throughput = 350 msec x 2000 bits = **700 bits.**

Variable bit rate of 4 kbit/sec up to 128 kbit/sec

Throughput = $(50E-3 \times 128E3) + (50E-3 \times 64E3) + (50E-3 \times 32E3) + (50E-3 \times 16E3) + (50E-3 \times 8E3) + (100E-3 \times 4E3) = \mathbf{12800 \text{ bits}}$

An increase in throughput of eighteen times.

 { Example ends }

A similar result has been proved [1.7] by way of an implementation of an adaptive bit rate modem, shown in Fig. 2.4. The detected RF signal shows the trail strength to be about -96 dBm, enough to support a 256 kbps data rate. This system has a maximum data rate of 64 kbps, so it jumps to that rate at the start of the data exchange. After about 400 msec, the S\N ratio has dropped to about 10 dB at 64 kbps, so the link is slowed to 32 kbps. As the signal continues to fade, the data rate is halved until, at 2 kbps, the signal is lost.

In this case, two thirds of the throughput (2394/3402) characters) occurred at the first (maximum) data rate. It is reported [1.7] that the typical trail supports 1/2 of the throughput at the highest bit rate, 1/4 at the second bit rate, 1/8 at the third rate, etc. If the system would have remained at the probe rate of 8 kb/s, the throughput would only have been 560 characters. The increase in throughput is therefore six times. The limits to this implementation of an adaptive bit rate modem are discussed in the following chapter.

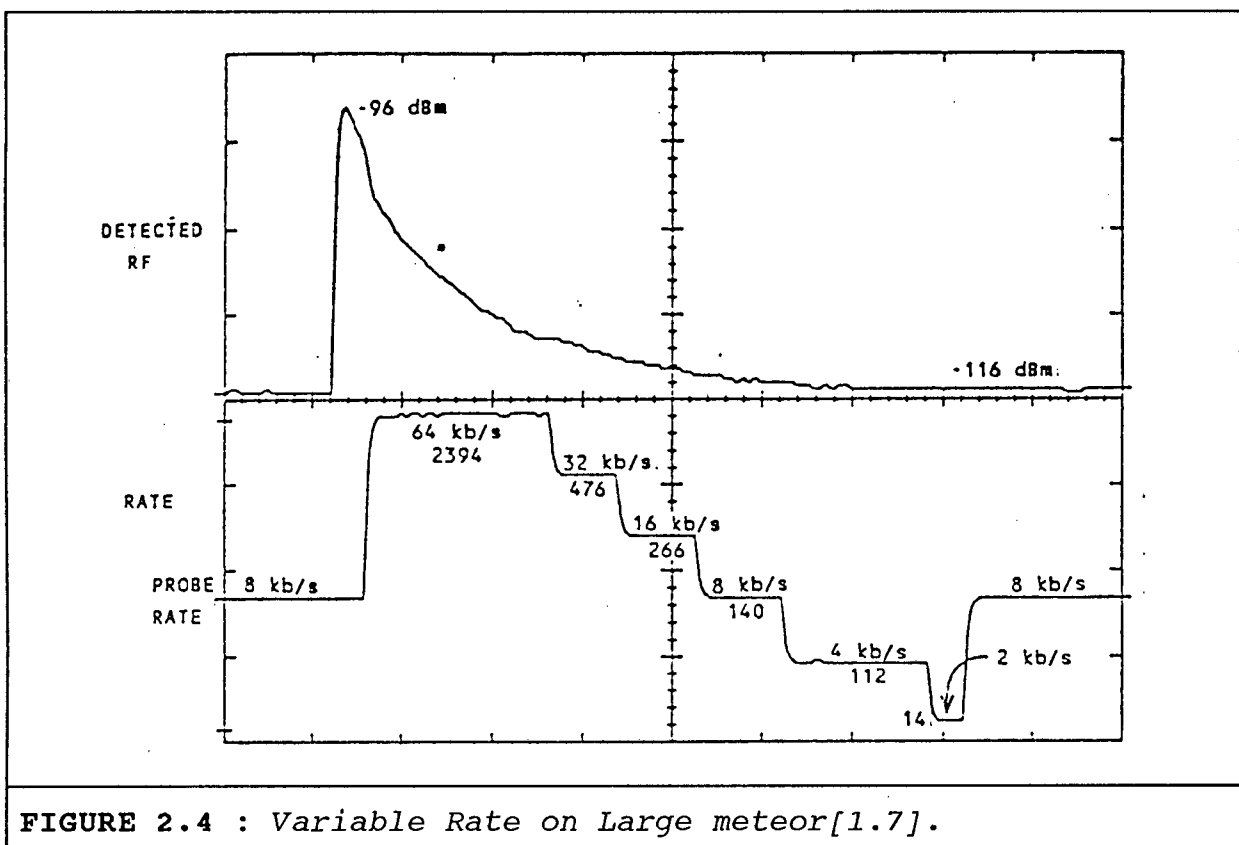


FIGURE 2.4 : Variable Rate on Large meteor[1.7].

2.4 ANALYTICAL COMPARISON OF THREE TYPES OF SYSTEMS [1.8]

The previous discussion of the optimum utilisation of a meteor trail, only considers one trail. The question still remains, whether the adaptive bit rate modem will show an increase in throughput over a constant bit rate system over many meteor trails? Since all trails are different in strength, duration and occurrence.

An analytical discussion of the improvement in this case has been done [1.8]. In this reference, three schemes are compared, namely; a variable adaptive bit rate scheme, a constant bit rate system and a constant bit rate system employing automatic message repeat request (ARQ). The discussion that follows briefly discusses the result of [1.8]. The ARQ system is omitted from the explanation. To make the comparison meaningful, the same channel model is used for all three systems.

CHANNEL MODEL [1.8]

1. The received signal power during one meteor burst can be represented as

$$P = P_m e^{-t/B} \quad W \quad (2.6)$$

where P_m is the peak power, and B is a time constant.

2. P_m and B are random variables for the ensemble of meteor bursts. For each individual burst, P_m and B are constants. the distributions of P_m and B are independent:

$f(a)$ = average number of meteor bursts per second with $P_m \geq a$.

$P_B(b)$ = probability of $B \geq b$.

3. The occurrences of meteor bursts are Poisson.

4. The frequency function $f(a)$ can be expressed as:

$$f(a) = K_1(a^{-n} - P_1^{-n}), \quad (0 < a \leq P_1) \quad (2.7)$$

where P_1 is the maximum value of the peak power, and $f(a) = 0$ for $a > P_1$. Equation (2.7) gives a probability density function

$$p(a) = ca^{-(n+1)} \quad \text{for } a \leq P_1 \\ = 0 \quad \text{for } a > P_1$$

which has been well documented in the literature for low density bursts [2.7]. The frequency function $f(a)$, is directly measurable and the variable n has been established empirically [2.8] to range between 0.57 and 0.96. The relationship between F and P_1 is approximated well by this equation, although the variation in n indicates the inconsistency in predicting meteor masses and meteor arrival. A value of 0.6 is used in this analysis.

Let E denote the received signal energy per bit for a prescribed signal to noise ratio (e.g. 10 dB). Let μ denote the bit rate, and P_0 denote a lowest designated pulse power. then

$$P_0 = \mu E \quad W \quad (2.8)$$

for a constant bit rate system. For a variable bit rate system (2.8) is replaced by

$$P_0 = \mu_0 E \quad W$$

where μ_0 is the lowest bit rate of the system. for both types of systems transmission ceases when $P < P_0$.

Once the channel model has been set up the the three mentioned cases are then analysed, namely the adaptive bit rate scheme, the constant rate scheme and the ARQ scheme. The procedure is as follows:

The number of bits in a burst is calculated, $N(a,b)$. For the constant bit rate case this equals the product of the bit rate and the trail duration. For the variable bit rate case, this depends on the bit rate which is assumed to vary in proportion with the received power. The number of bits in a burst is the result of an integration of the received power above a threshold, for the duration of the trail. The throughput rate equation (average bits/sec) is given as

$$N(a,b) = \mu t_1 = \mu b \ln \frac{a}{P_0} \quad (2.11)$$

for the constant bit rate case, and

$$N(a,b) = \frac{1}{E} \int_0^{t_0} P dt \quad (2.12)$$

$$\Rightarrow = \frac{b}{E} (a - P_0)$$

for the variable bit rate case. Once the throughput has been calculated for any trail, as a function of a , the received power and b , the duration of the burst, the average throughput rate per burst, N , is calculated,

$$N = \int_0^\infty \int_{P_0}^{P_1} N(a,b) df(a) dP_b(b) \quad (2.13)$$

The result of the integration is an equation of throughput rate, N , in terms of the specific throughput $f(n,x)$ where $x = P_0/P_1$.

$$f(n,x) = \frac{x}{n} (x^{-n} - 1 + n \ln x)$$

for the constant rate modem and

$$f(n,x) = \frac{n}{1-n} - \frac{x^{1-n}}{1-n} + x$$

for the variable bit rate modem. A plot of $f(n,x)$ for the three cases is shown in Fig. 2.5 (an explanation for the third case has been omitted), which indicates the improvement in throughput obtained with an adaptive bit rate scheme over the other two schemes.

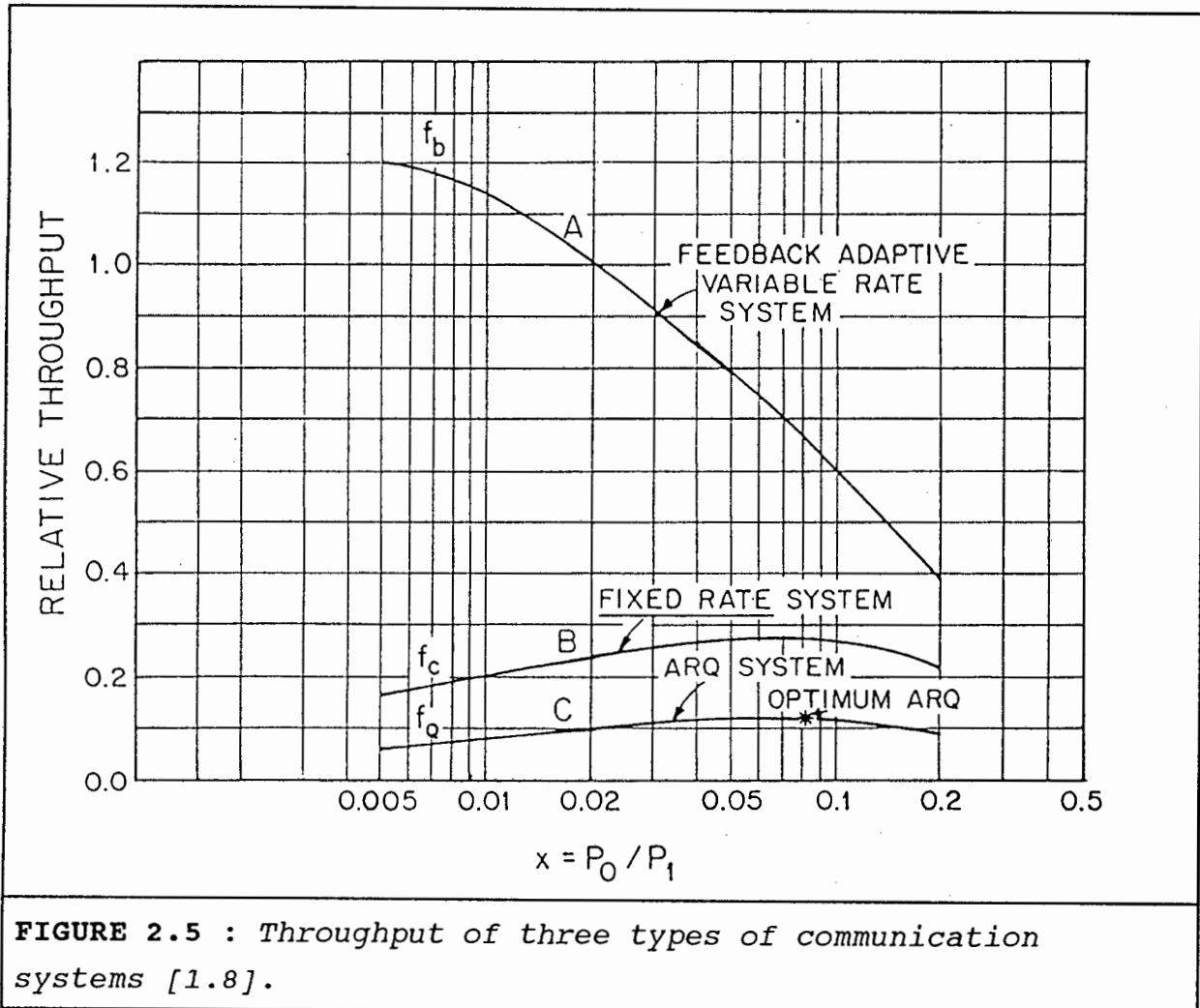


FIGURE 2.5 : Throughput of three types of communication systems [1.8].

2.5 PRACTICAL OPERATIONAL LIMITS

The two shortcomings of the theory of the adaptive bit rate modem of sub-section 2.4 are :

1. The received trail shape is limited to a decaying exponential, which is not the case for many recorded trails [2.1].

2. It is assumed that the adaptive bit rate modem varies continuously with the received signal-to-noise ratio. However, it is impractical to have a continuously varying bit rate. Such a system would forever be changing bit rate and would have no time to synchronise or demodulate data. Therefore equation (2.12), used to calculate the throughput per burst, when applied to a practical adaptive bit rate modem, should not be a continuous integral, but rather a discrete summation. The adaptive bit rate modem then switches between discrete bit rates at certain absolute received power levels. This is shown as follows:

$$N(a,b) = \frac{1}{E} \sum_{t=0}^{t_0} P_t \Delta t \quad (2.14)$$

the graph of variable bit rate of Fig. 2.5 will not show the same large improvement over a constant bit rate system. The improvement may still exist, but will depend on the discrete steps chosen in the summation.

Other practical considerations are that channel utilisation can also be degraded by the practical modem limits. For example, lock up times of synchronised loops and rate change circuits. The increase in throughput is much less than would seem from the above theoretical predictions. The practical limits of the adaptive bit rate modem are described as follows:

The time taken from the moment the receiver receives sends a command for a new bit rate, until the receiver locks onto a new rate is called the rate change delay time, RCD, calculated as :

$$RCD = t_{rd} + t_{cd} + t_{td} + t_{cd} + t_{rtd} \quad \text{sec.}$$

Where :

t_{rd} = time taken from the moment the receiver measures a fade until the transmitter in the same unit transmits this information back to the first transmitter.

t_{cd} = time taken for message to reach destination over meteor scatter path (this delay occurs twice as the message is relayed in a feedback type loop).

t_{td} = time taken from the instant the message to change rate is received until the transmitter actually changes rate.

t_{rld} = time taken for receiver to lock onto the new rate from the arrival of the command for the new rate. This is the lock up time of the control circuitry.

This sets a minimum delay between bit rate changes, RCD_{min} . Therefore the modems will operate at each bit rate for a minimum time even if the signal fade is much faster than this minimum time.

Beyond the control of the modem is the transmission of measurements regarding bit rate in the feedback path provided by the full duplex arrangement, t_{rd} and t_{td} . This must be done with minimum delays allowing fast response of the modem to changes in the received channel fade on both sides of a link. Also, the time taken to transmit this message, t_{cd} , is roughly calculated as being the time taken for electromagnetic radiation to traverse a distance of 1500 Km ,

$$t_{cd} = \frac{1.5 \times 10^6}{3 \times 10^8 \times 0.9} \text{sec} = 5.5 \text{msec}$$

The speed of propagation is less than the speed of light by a velocity factor taken as 0.9 here. This time is not accurate but gives an indication as to the time that is lost from sending a message to receiving a message. Also, the distance between two stations is a variable.

The speed of the modem to switch to the new bit rate, at the receiver, is given by t_{rld} . For example, if a trail only lasts for 1 sec, and three rate changes are required during this period, 333 msec are available for communicating at each bit

rate. The RCD must not exceed, say 40 msec. The practical limitations can be reduced to some extent by the modem design. Hence the specifications given in chapter one on carrier lock up times and modem synchronisation.

2.6 CONCLUSION

It has been predicted that high speed communications can be accommodated over a meteor scatter link [1.6]. It has been predicted that an adaptive bit rate modem will offer higher throughput over constant bit rate modems [1.8] and indeed proved to be the case [1.7].

The effect of the amplitude fade dominates over the effect of the phase incoherence. The channel bit rate capacity is therefore determined by the received signal-to-noise ratio. A consequence of this is, that the upper bit rate limit of 1 Mbit/sec, that is set by phase incoherence on large meteors can only be achieved if the received S/N during the trail at 1 Mbit/sec is sufficiently large.

The meteor scatter channel can therefore be described as a power limited environment.

The *natural* channel can be modelled as having a time varying characteristic. Both the amplitude response and phase response changes during the existence of a link. However, the channel will be assumed to have a flat amplitude spectrum and a linear phase response over the finite bandwidth of interest during the useful existence of the trail. The following chapter will explain the modulation techniques that are available and how a selection to use one technique has been made.

The quadrature arm is identical to a phase locked loop and performs the loop tracking control. The multiplier-arm filter is the phase detector with units V/rad. The input carrier amplitude, local oscillator amplitude, multiplier gain and low pass filter gain are combined into a phase detector gain having units of V/rad. K_{PD1} rad/V is thus a function of the voltage levels of the local oscillator as well as the input signal. To eliminate this dependency, the input voltage and local oscillator voltage are set as constants.

This is written as

$$K_{PD1} = \frac{\sqrt{2}}{2}(\bar{V})(K_{m2}K_{f2}) \quad V/rad$$

Equations (C-17) and (C-16) are multiplied at the linear loop multiplier to give the following result:

$$V_{m3}(t) = V_{mi}V_{mq}(t)K_{m3} \quad V$$

$$= \frac{\sqrt{2}}{2}(\bar{V})[K_{PD1}K_{m1}K_{f1}K_{m3}(\hat{m}(t))^2(\Delta\theta)] \quad V \quad (C-18)$$

K_{m3} is the linear multiplier gain with units of V^{-1} . It assumed that the data is perfectly recovered by the arm filters such that $(\hat{m}(t))^2 = 1$

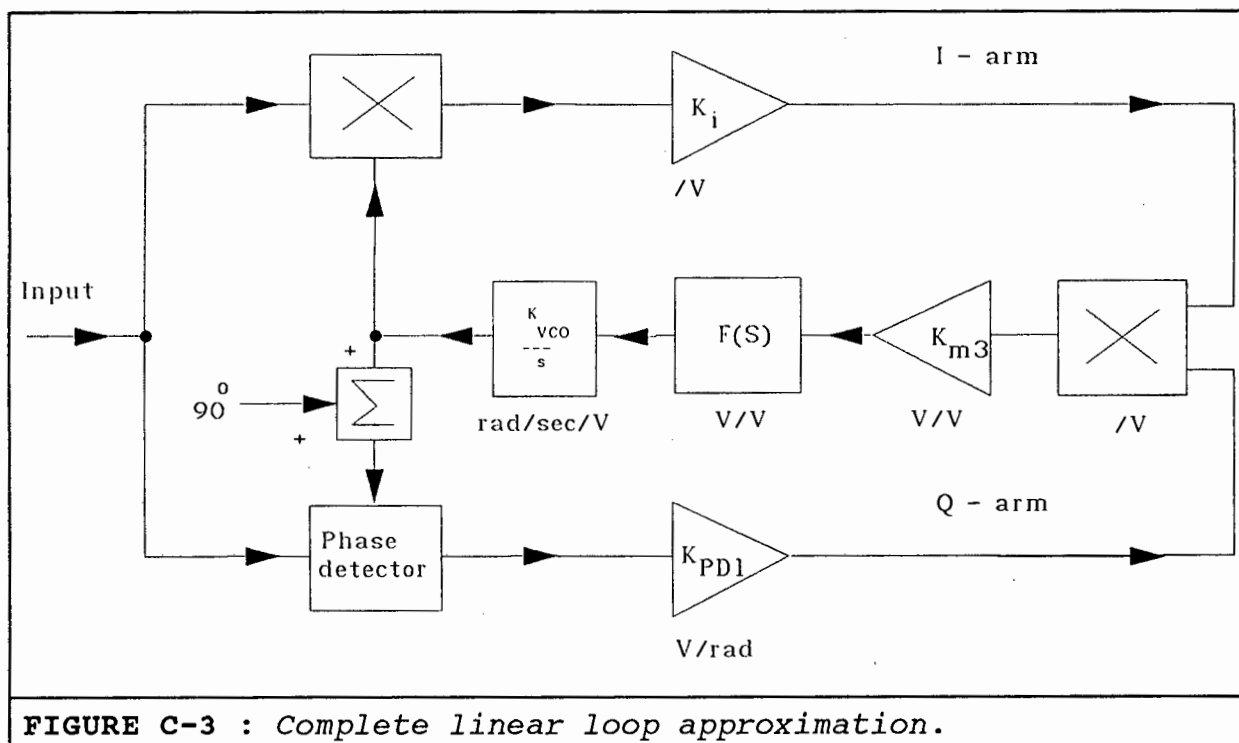


FIGURE C-3 : Complete linear loop approximation.

The in-phase arm remains essentially unity, and the quadrature-phase arm performs the tracking, the gain of the in-phase multiplier-low pass filter is not V/rad but V^{-1} . The loop multiplier is a linear multiplier and is not further simplified.

Equation (C-18) becomes:

$$V_{m3}(t) = (\hat{K})(\Delta\theta) \quad (V) \quad (C-19)$$

Where

$$\hat{K} = \frac{\sqrt{2}}{2} (\hat{V}) [K_{PD1} K_{m1} K_{f1} K_{m3}] \quad (C-20)$$

Applying this to the loop filter, the output dc control voltage is:

$$V_{dc}(s) = V_{m3}(s) * F(s) \quad V \quad (C-21)$$

This is applied to the VCO, the result is :

$$V_{VCO}(s) = V_{m3}(s) F(s) \left(\frac{K_{VCO}}{s} \right) \quad (C-23)$$

$$V_{VCO}(s) = (\hat{K})(\Delta\theta) F(s) \left(\frac{K_{VCO}}{s} \right) \quad (C-24)$$

The VCO integrates the dc voltage and the output is the local oscillator phase, therefore :

$$\theta_o(s) = V_{VCO}(s)$$

and from (C-15) above :

$$\Delta\theta = \theta_c - \theta_o$$

Giving :

$$\theta_o(s) = (\hat{K}) F(s) \left(\frac{K_{VCO}}{s} \right) (\Delta\theta_o(s) - \Delta\theta_c(s)) \quad (C-25)$$

The open loop transfer function is given as:

$$H_o(s) = (\hat{K}) F(s) \left(\frac{K_{VCO}}{s} \right) \quad (C-26)$$

The open loop gain is completely given as

$$k_{ol} = \frac{\sqrt{2}}{2} (\hat{V}) K_{m3} \cdot K_{PD1} \cdot F(0) \cdot K_{m1} \cdot K_{f1} \cdot K_{VCO} \quad (C-27)$$

which has units of sec^{-1} . The loop filter dc gain, $k_{f1} = F(0)$. The open loop transfer function of the Costas loop resembles that of the simple phase-locked Loop. The units around the loop are given. The linear approximation of the loop has been redrawn as shown in Fig. C-4.

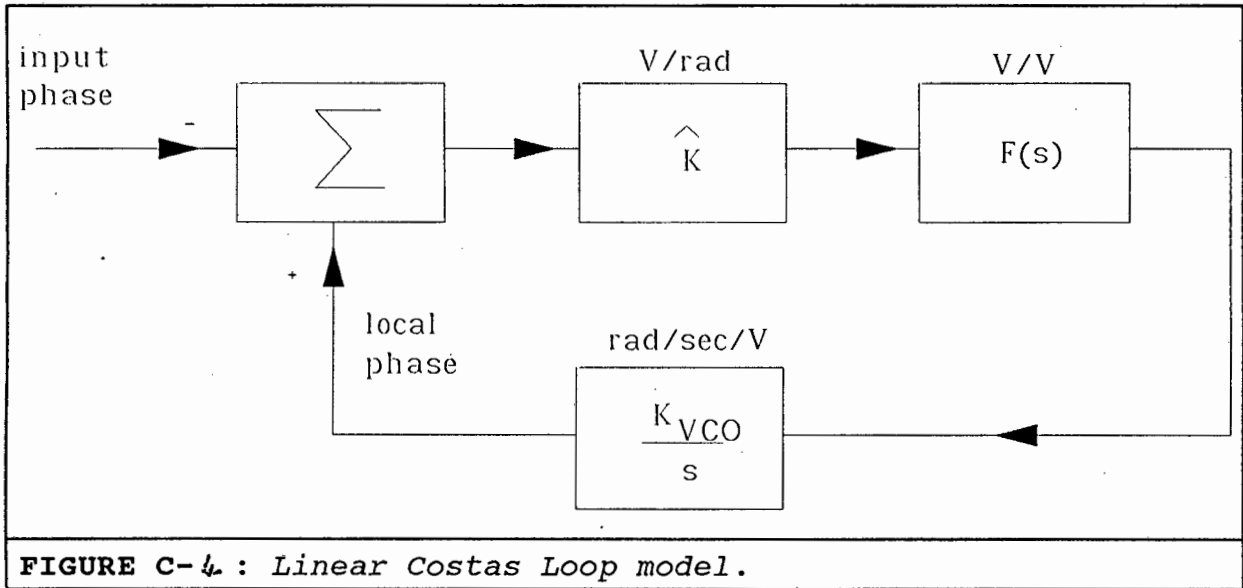


FIGURE C-4 : *Linear Costas Loop model.*

The closed loop transfer function can then be written as:

$$T(s) = \frac{\theta_o(s)}{\theta_c(s)} = \frac{\hat{K} K_{VCO} F(s)}{s + \hat{K} K_{VCO} F(s)} \quad (C-28)$$

This is the complete closed loop transfer function and the Costas loop may now be analysed using Phase-locked loop theory. The phase locked loop theory is given in appendix B.

APPENDIX D

SWITCHED CAPACITOR FILTER DESIGN

DESIGN EQUATIONS

Cut off frequency, f_o :

$$f_o = \frac{f_{CLK}}{50} \times \left(\sqrt{\left(\frac{R_2}{R_4} + 1 \right)} \right)$$

Q = Quality factor:

$$Q = \sqrt{\frac{R_2}{R_4}} \times \left(\frac{R_3}{R_2} \right)$$

Highpass Gain as $f \rightarrow f_{CLK}/2$:

$$H_{OHP} = -\frac{R_2}{R_1}$$

Bandpass Gain at $f = f_o$:

$$H_{OBP} = -\frac{R_3}{R_1}$$

Lowpass gain as $f \rightarrow 0$:

$$H_{OLP} = -\frac{R_4}{R_1}$$

An important characteristic of sampled-data systems is their effect on signals at frequencies greater than the sampling or clock frequency applied to it. The sampling frequency must be at least twice the highest spectral component in the input spectrum to the filter otherwise aliasing will occur. To avoid aliasing, an anti-aliasing low pass filter can be included just before the filter to eliminate the very high frequency components like the double frequency term which result at the output of a double balanced multiplier. This will occur at 1.4 Mhz in this case. Passive RC filters have been used with $R = 6k\Omega$ and $C = 100$ pF. This gives a -3dB frequency of $f_{-3dB} = 265$ Khz which is found to be adequate.

The function of the switched capacitor filter is to further limit the spectrum to the bit rate frequency, which eliminates noise.

The four resistors have values given in table D-1. The designed parameters are given in table D-2. The switched capacitor circuit is shown in Fig D1.

R_1 <small>kΩ</small>	R_2 <small>kΩ</small>	R_3 <small>kΩ</small>	R_4 <small>kΩ</small>
10	27	10	10
TABLE D-1 : Resistor values of switched capacitor filter.			

f CLK	f _o	Q	H OHP	H OBP	H OLP
3500 Khz	135 Khz	0.608	- 2.7	-1	- 1
1750 Khz	68 Khz	0.608	- 2.7	-1	- 1
875 Khz	34 Khz	0.608	- 2.7	-1	- 1
437.5 Khz	17 Khz	0.608	- 2.7	-1	- 1
218.75 Khz	8.4 Khz	0.608	- 2.7	-1	- 1
109.375 Khz	4.18 Khz	0.608	- 2.7	-1	- 1

TABLE D-2 : Table of the six switched capacitor filter parameters.

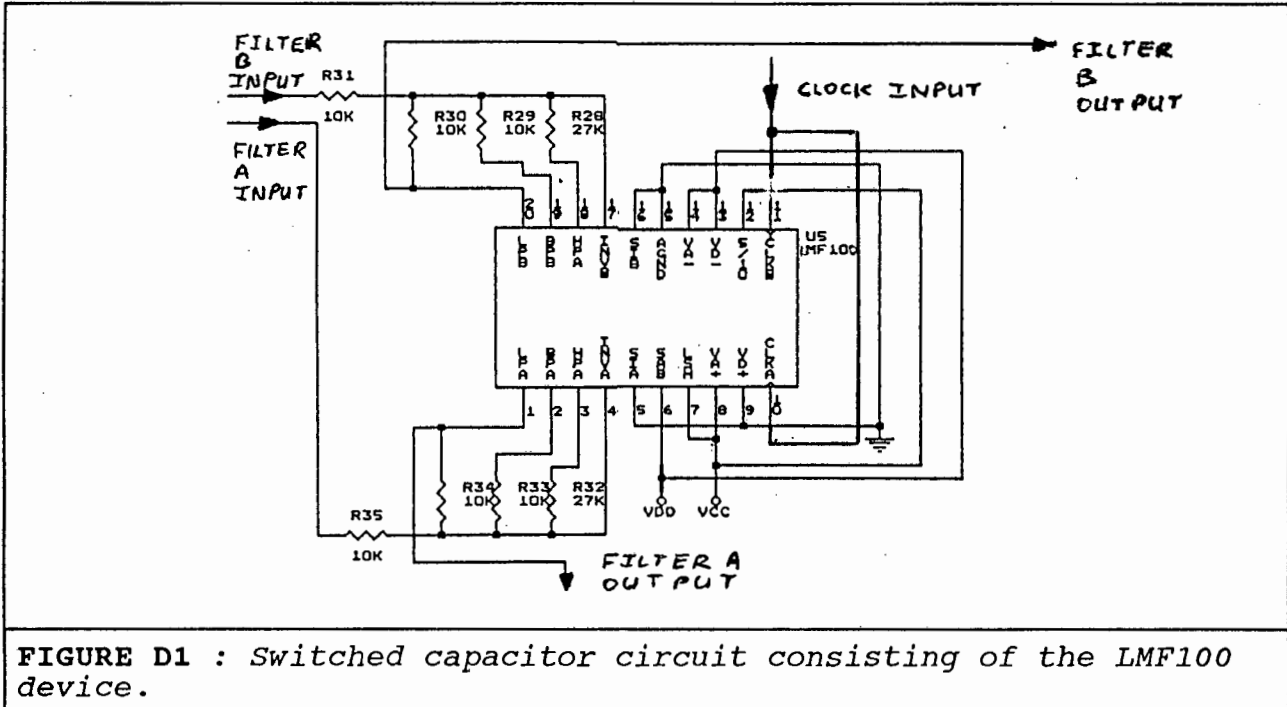
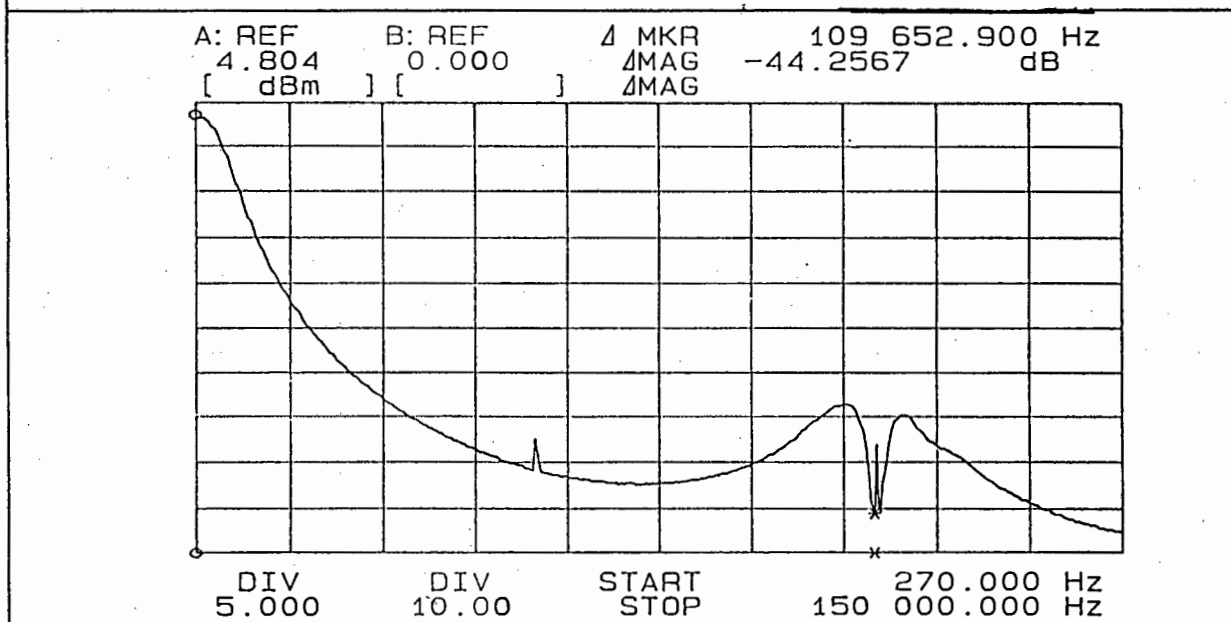
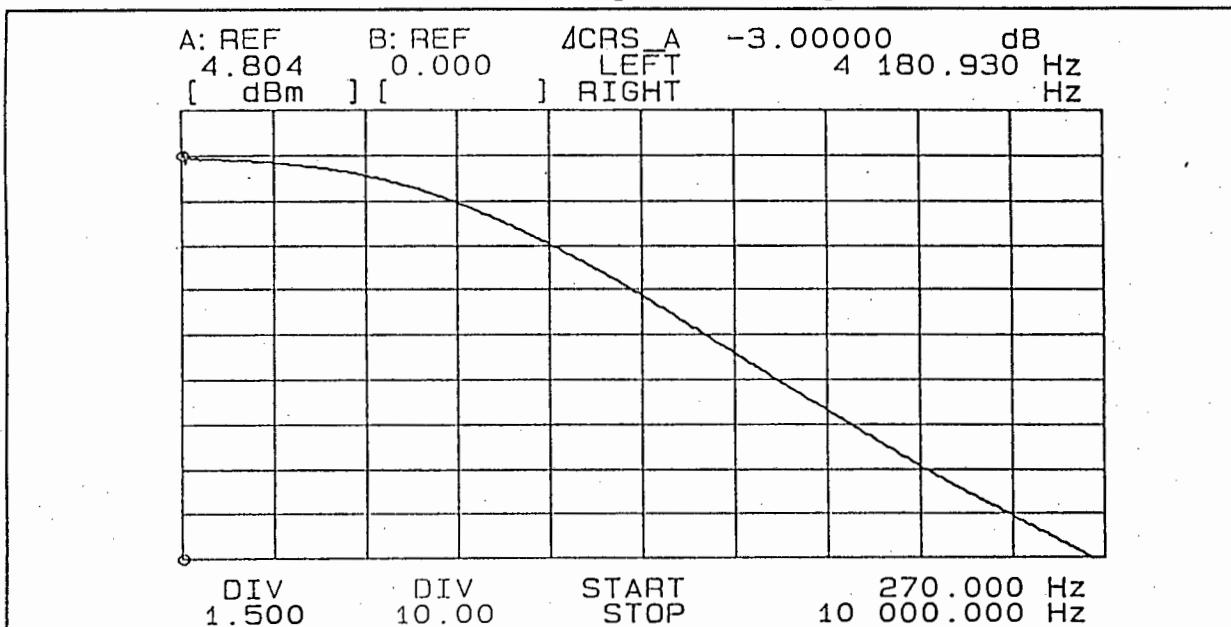


FIGURE D1 : Switched capacitor circuit consisting of the LMF100 device.

The following six pages illustrate the phase and amplitude response of each of the arm filters, as selected by applying the appropriate clock frequency. The amplitude response has been obtained on the 4195A Hewlett Packard Network/Spectrum analyser and using the 4741 plotter. The amplitude response is given in two views, a close up of the passband in one view and the stop band in the other. This is to show the sampling frequency of the applied clock of each filter. This is noticed as the discrete component.

F = 4 khz , Amplitude Response



F = 4 khz , Phase Response

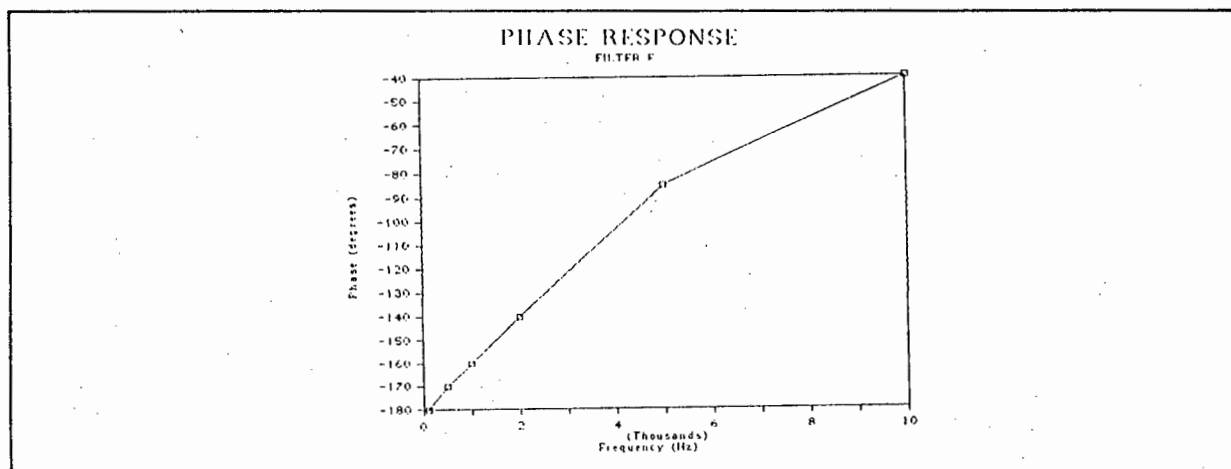
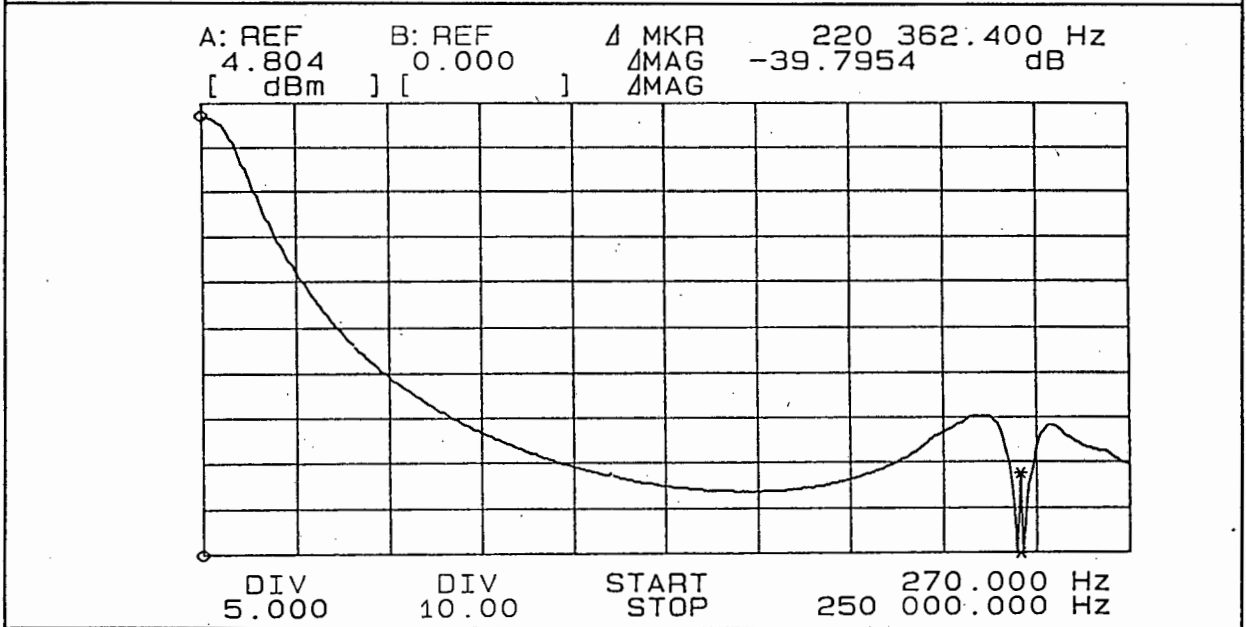
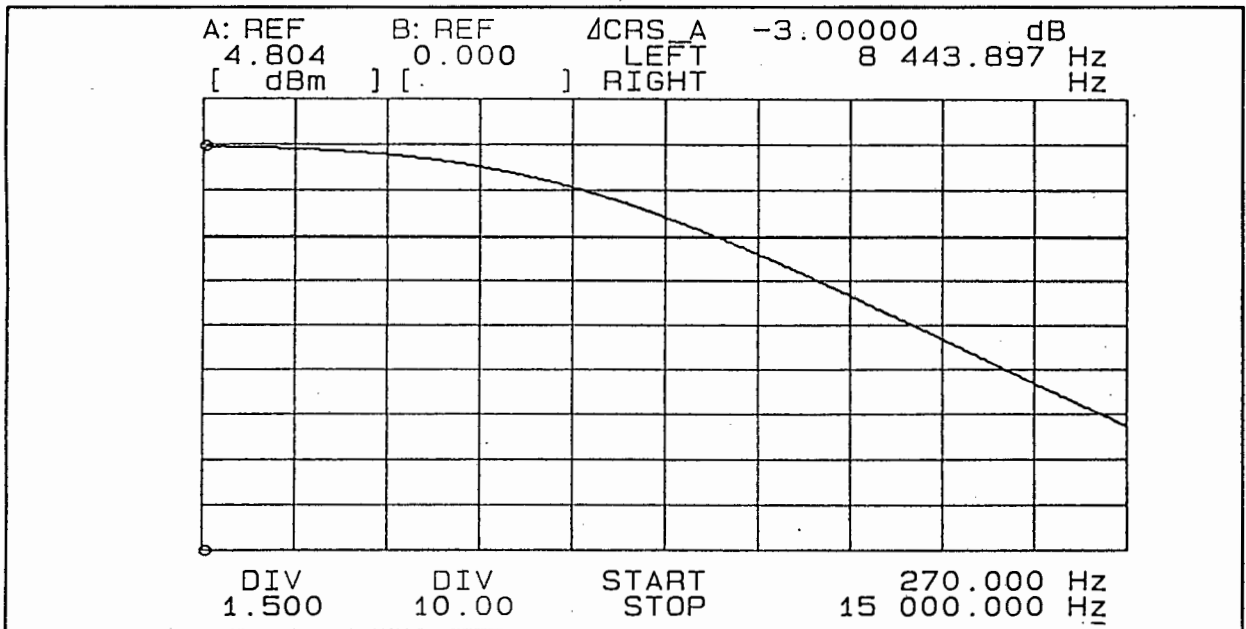
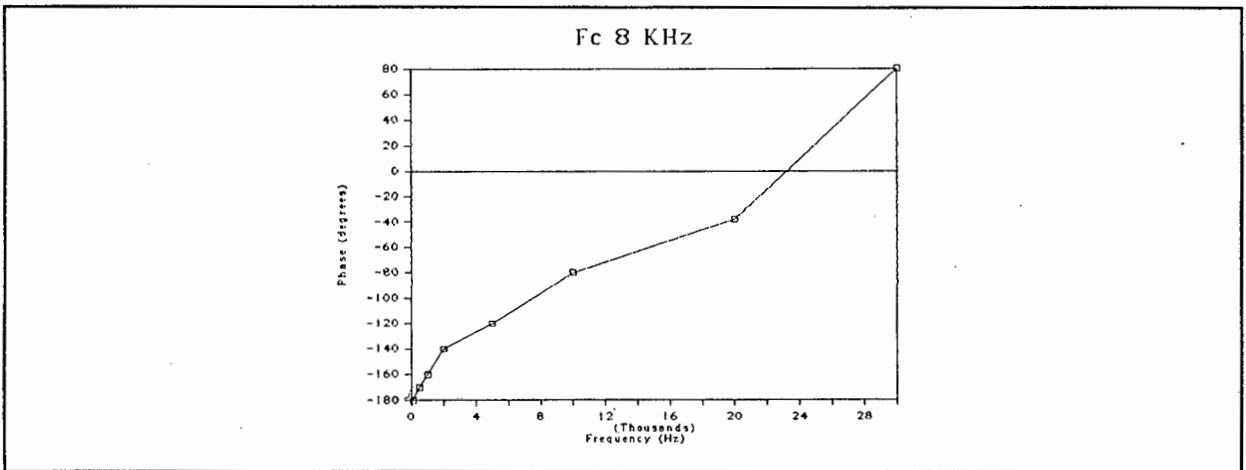


FIGURE D2 : AMPLITUDE AND PHASE RESPONSE OF FILTERS.

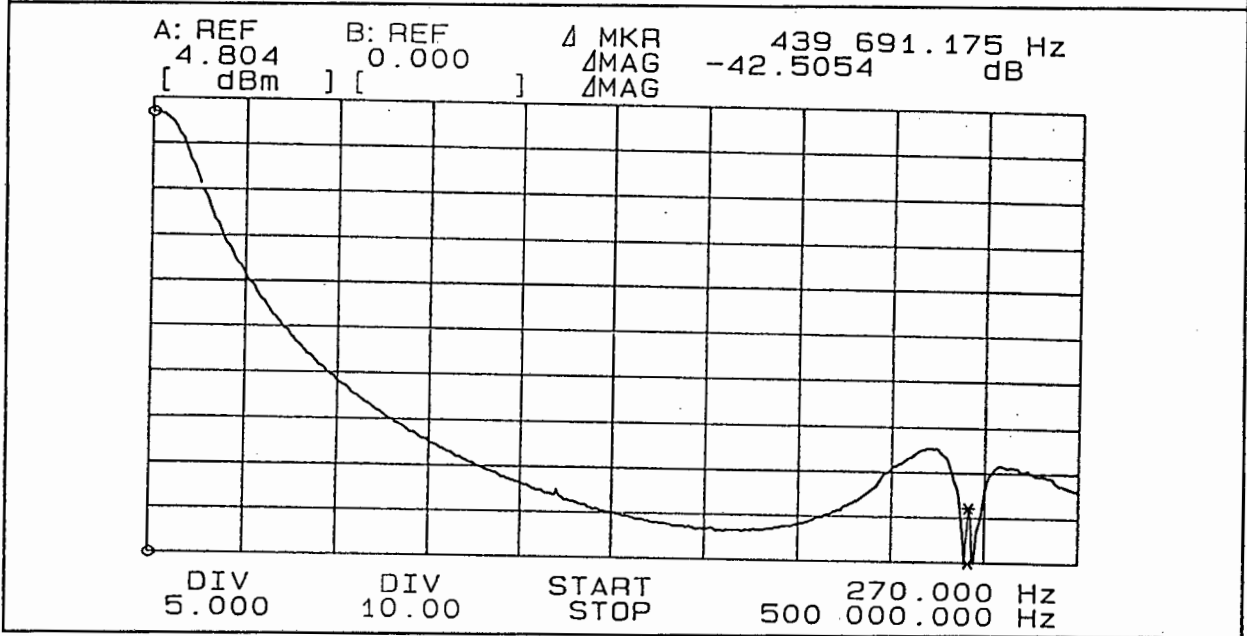
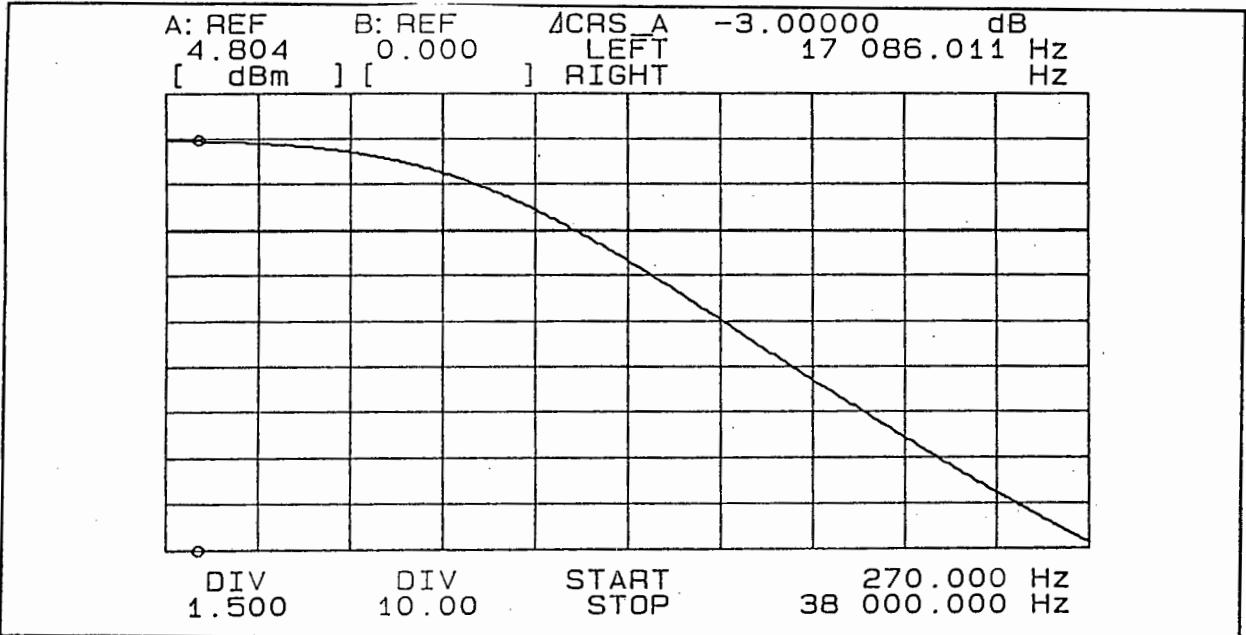
F = 8 khz , Amplitude Response



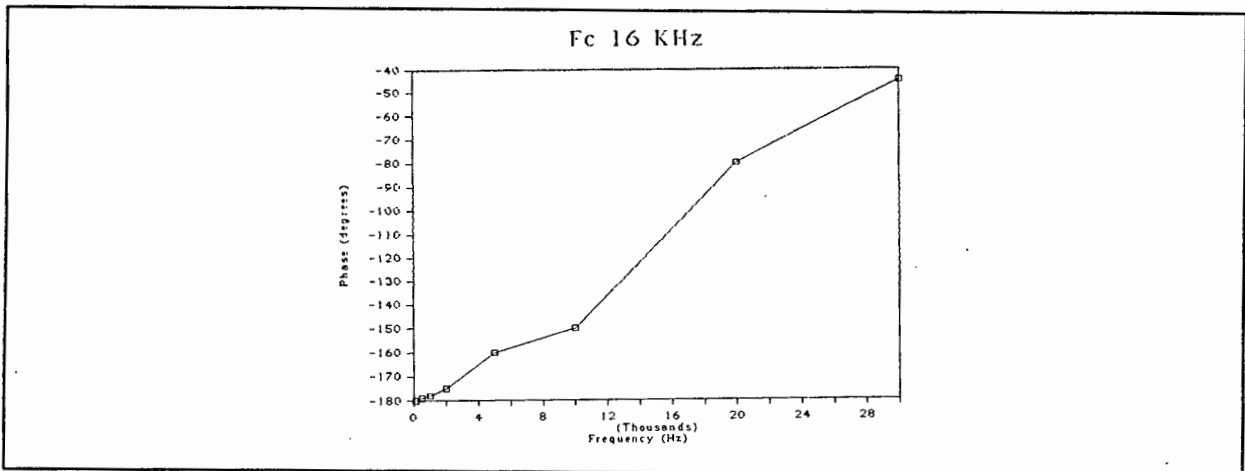
F = 8 khz , Phase Response



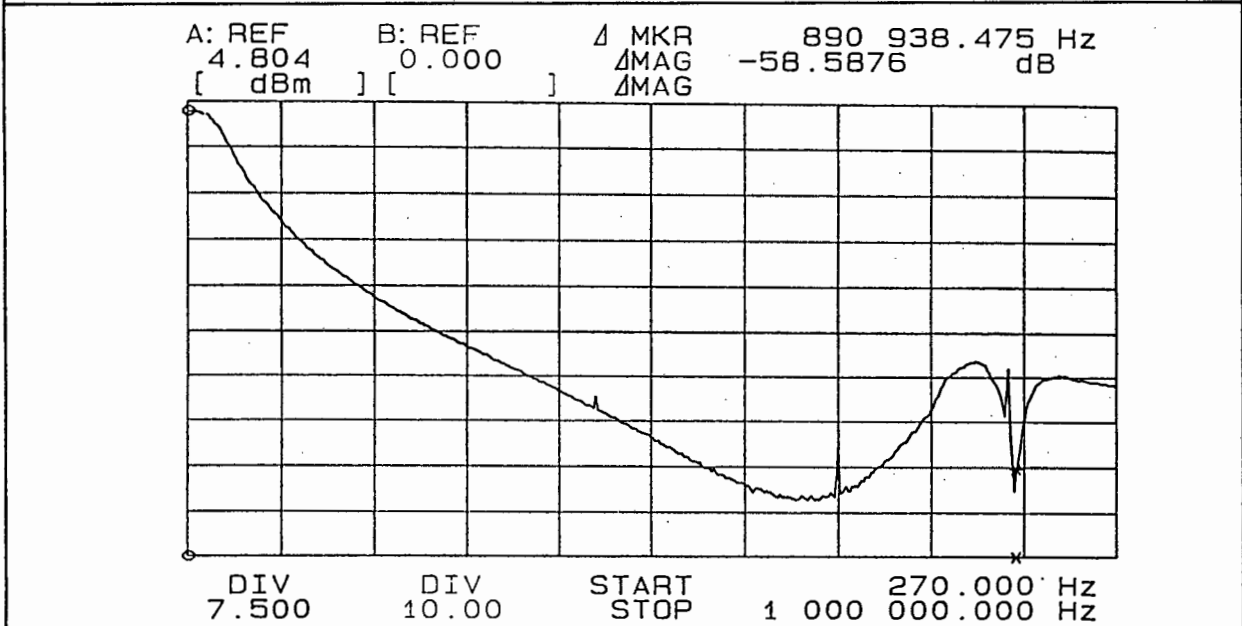
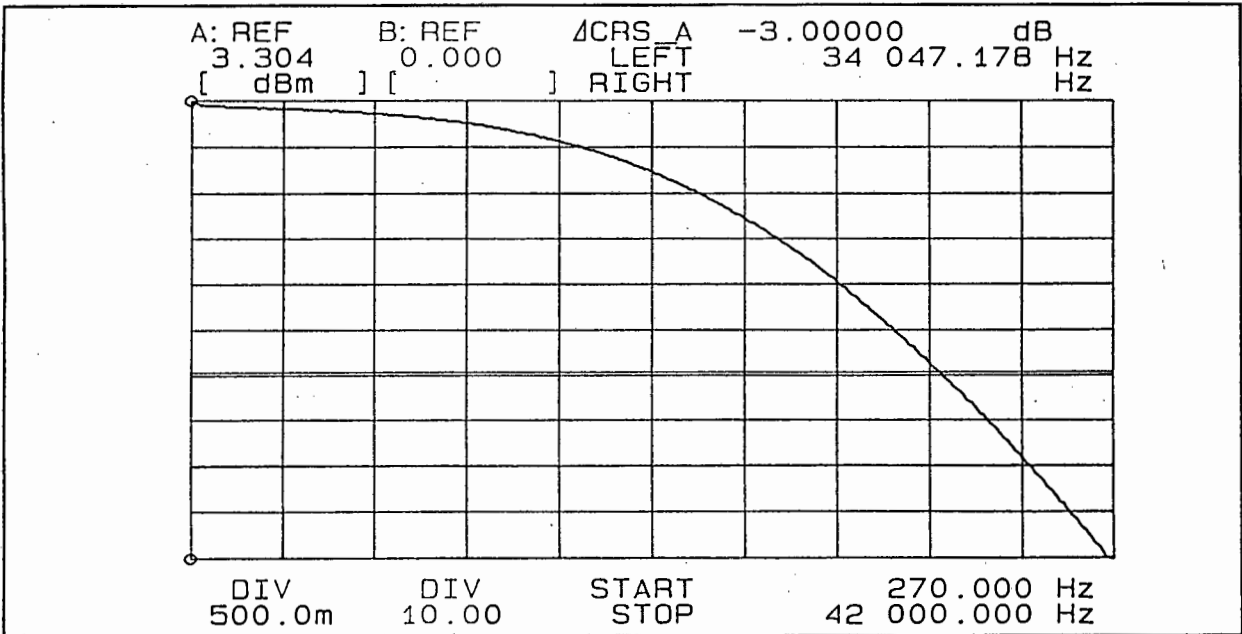
F = 16 khz , Amplitude Response



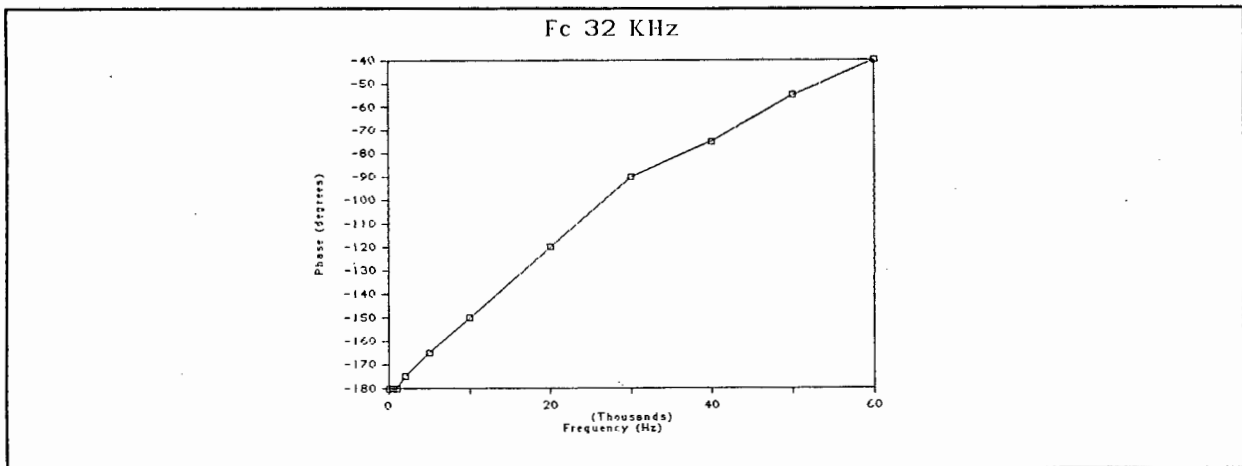
F = 16 khz , Phase Response



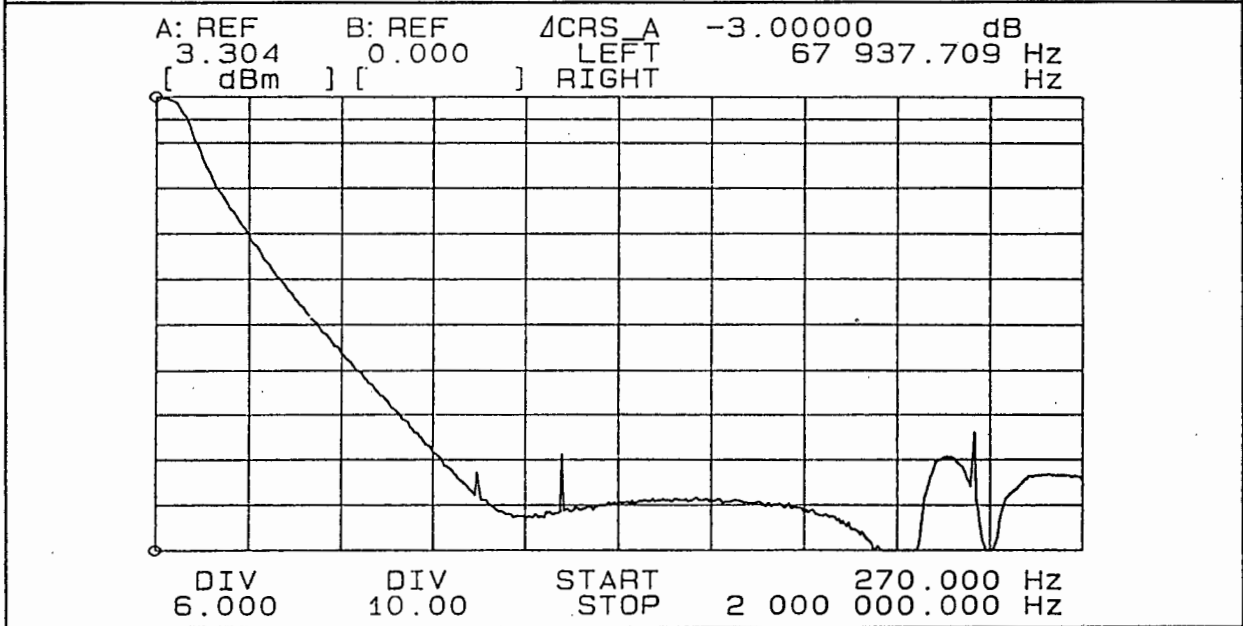
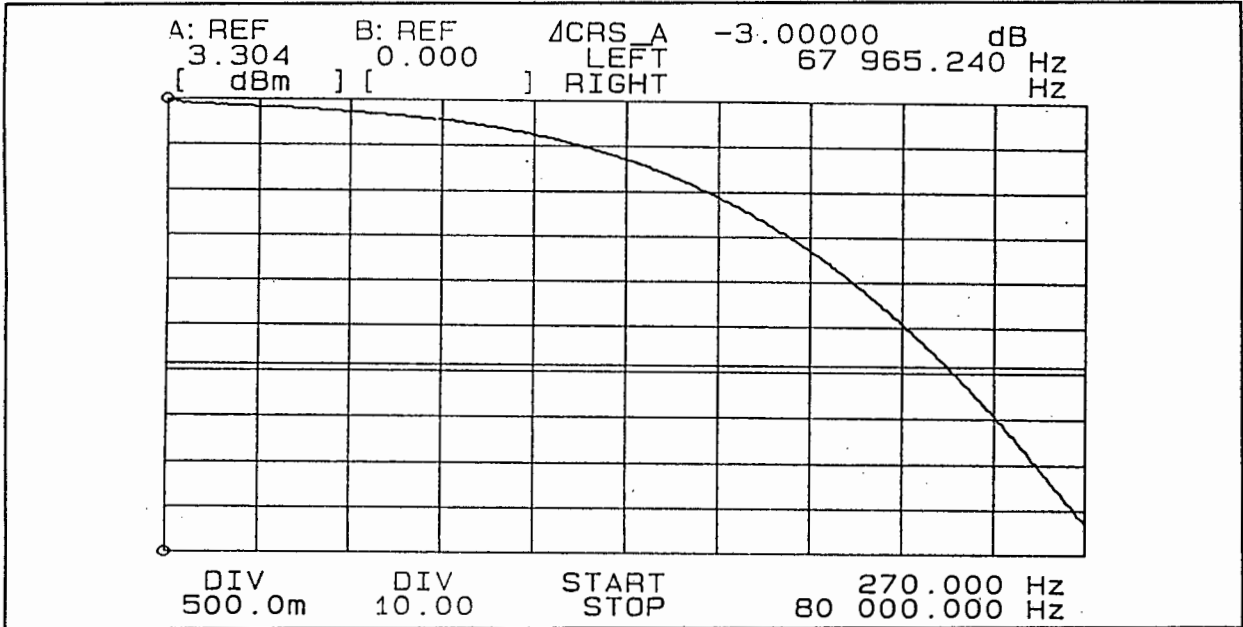
F = 32 khz , Amplitude Response



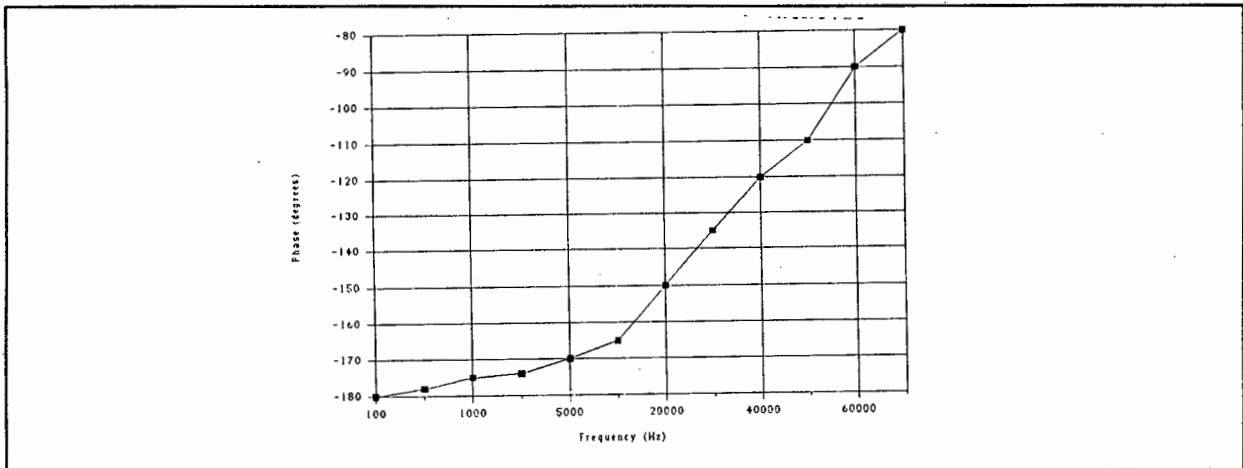
F = 32 khz , Phase Response



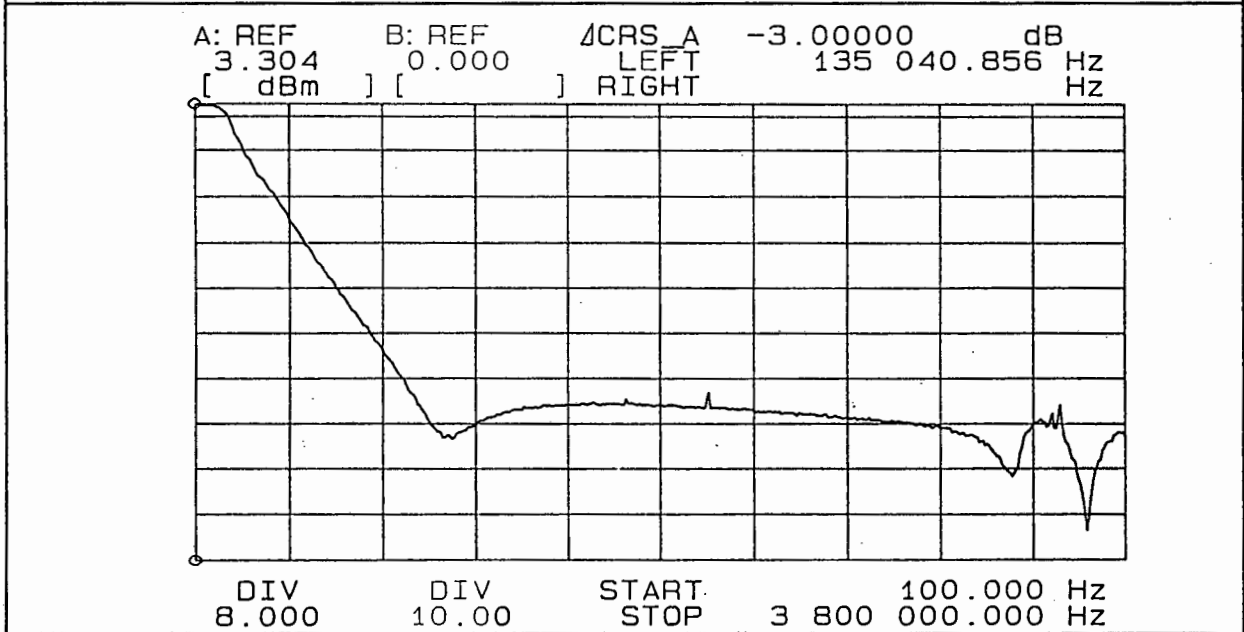
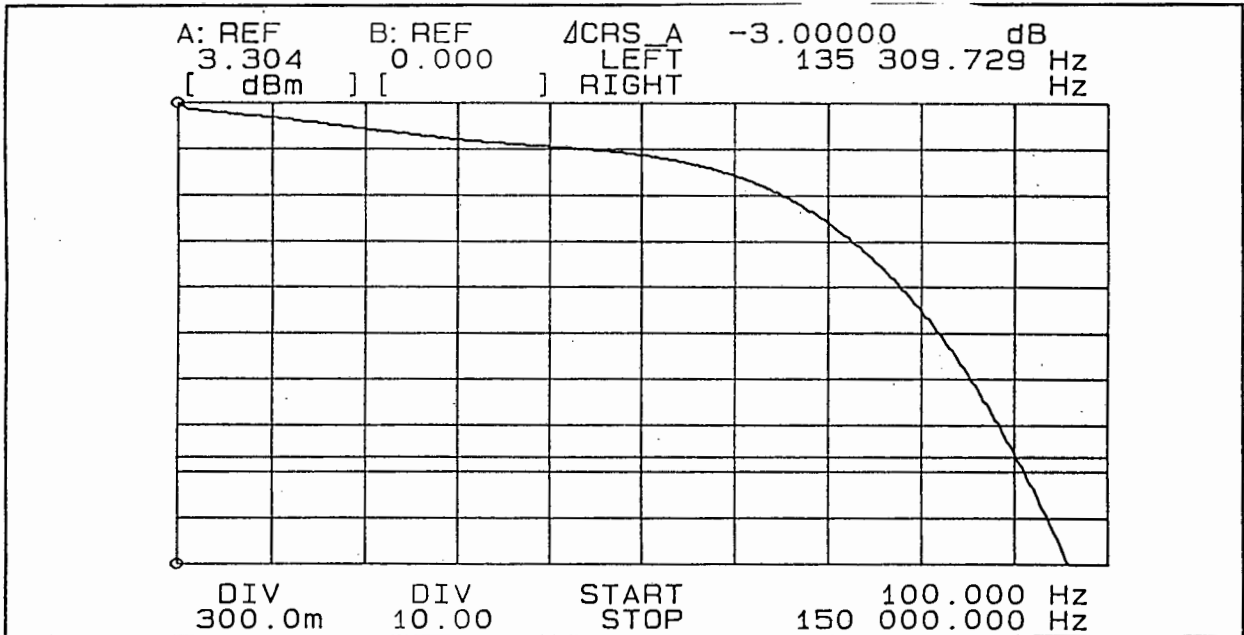
F = 64 khz , Amplitude Response



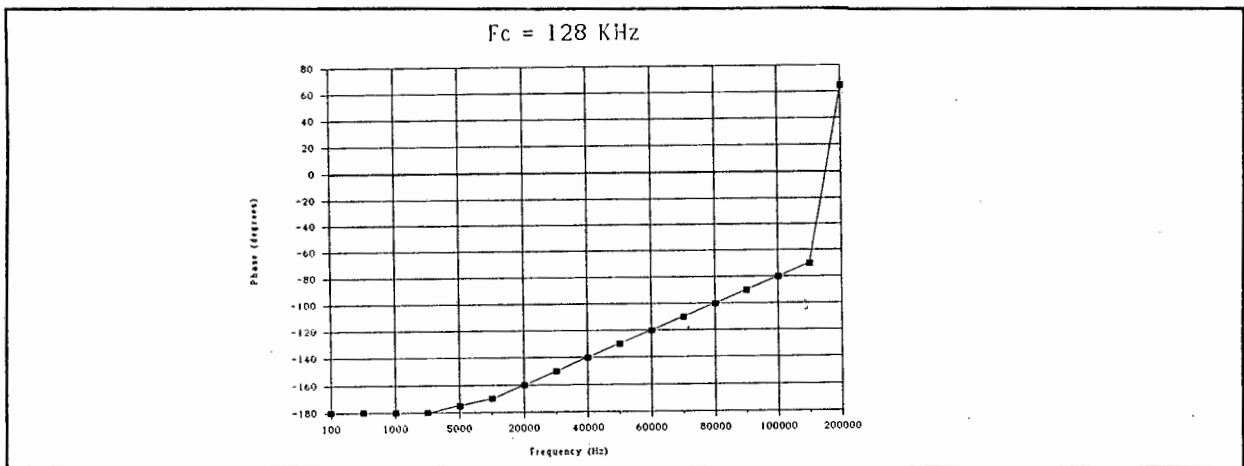
F = 64 khz , Phase Response



F = 128 khz , Amplitude Response



F = 128 khz , Phase Response



APPENDIX E

PASSIVE BAND PASS FILTERS

1.1 CIRCUIT DIAGRAM OF SIX PARALLEL FILTERS with MULTIPLEXER

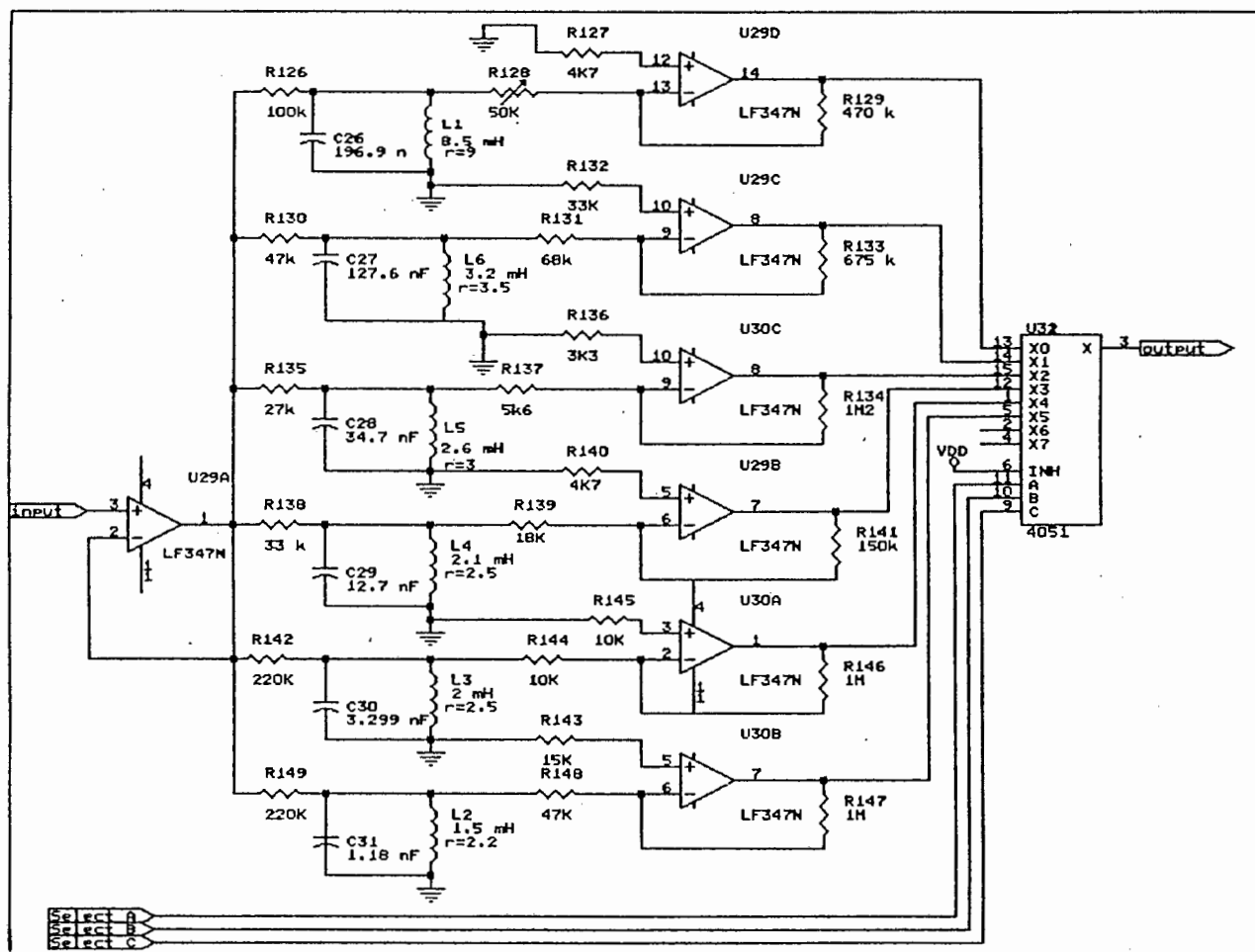
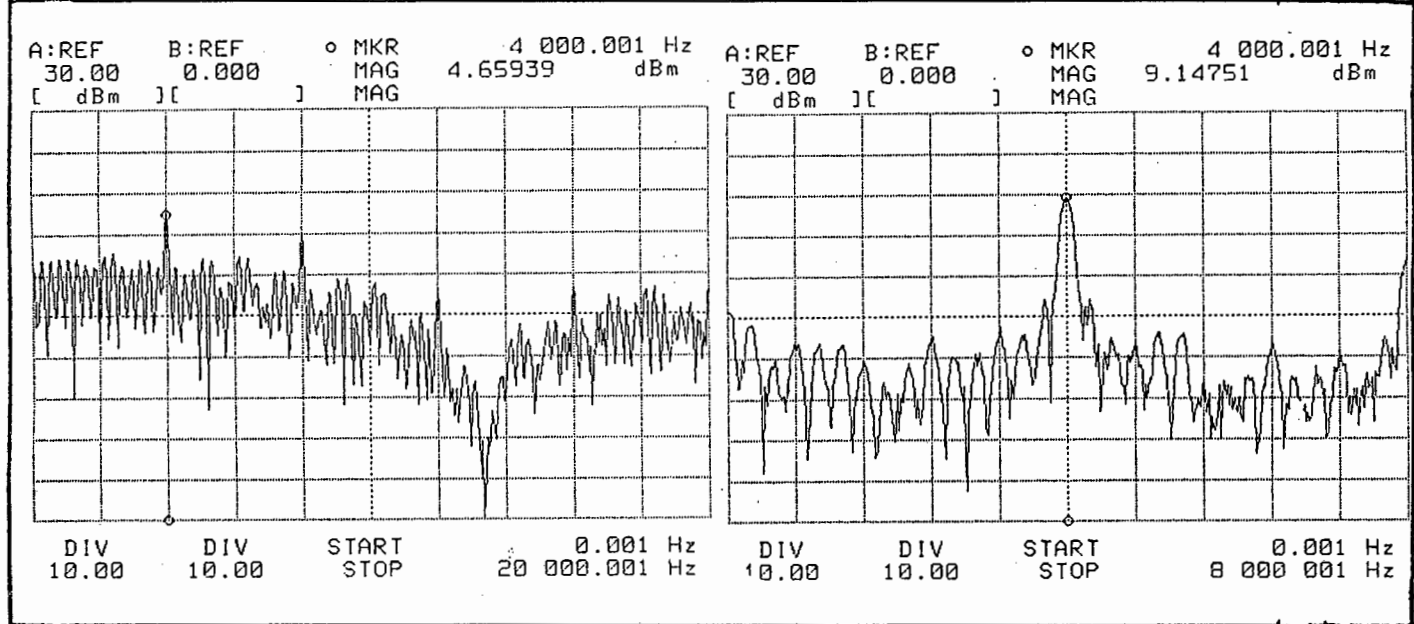
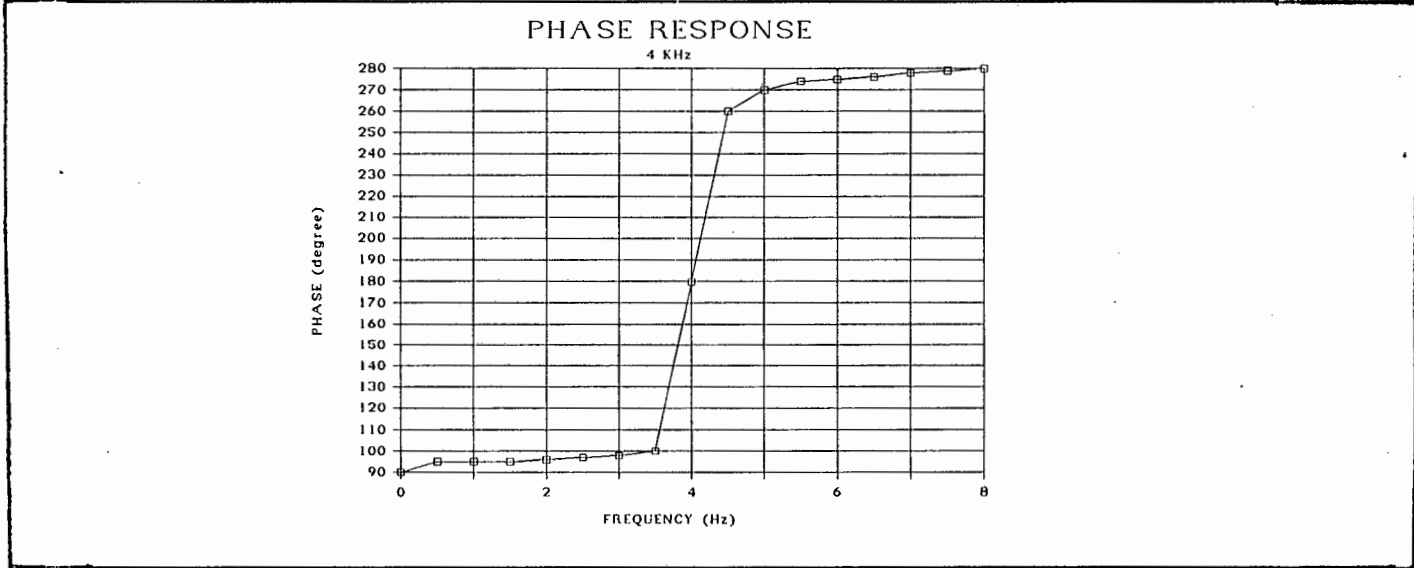
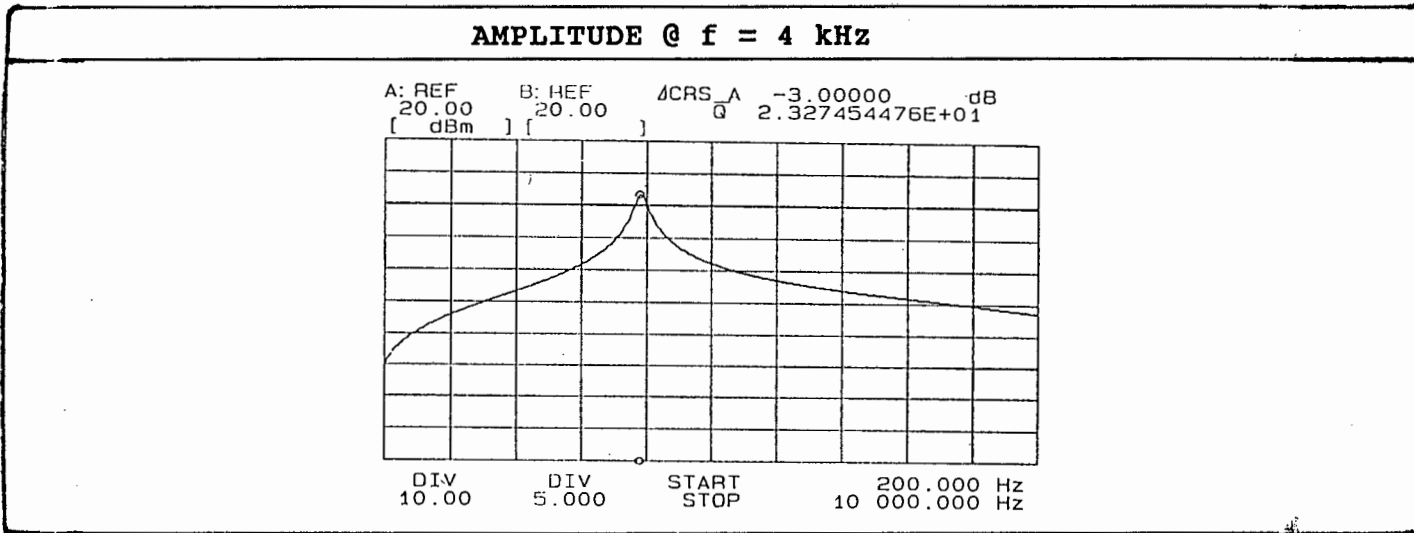


FIGURE E1 : CIRCUIT DIAGRAM OF PASSIVE BAND PASS FILTERS.

1.2 AMPLITUDE AND PHASE RESPONSE

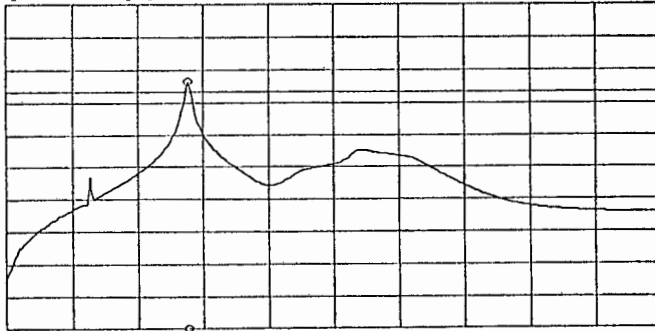


Input and output spectrum

FIGURE E2 : AMPLITUDE AND PHASE RESPONSE OF FILTERS WITH INPUT AND OUTPUT SPECTRA.

AMPLITUDE @ f = 8 kHz

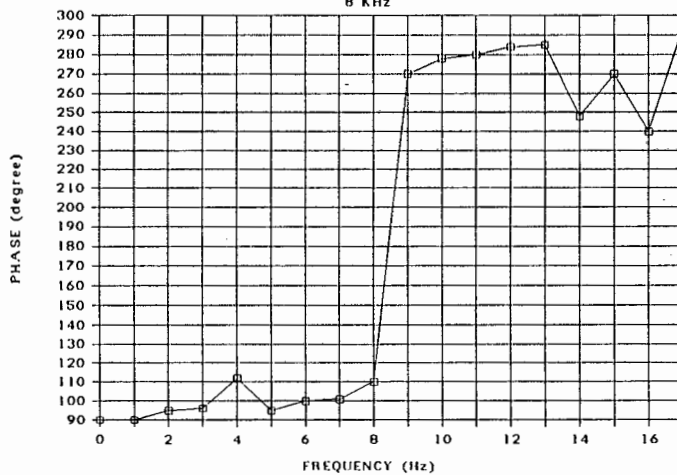
A: REF 20.00 [dBm] B: REF 20.00 [] ΔCRS_A -3.00000 dB Q 3.559232567E+01



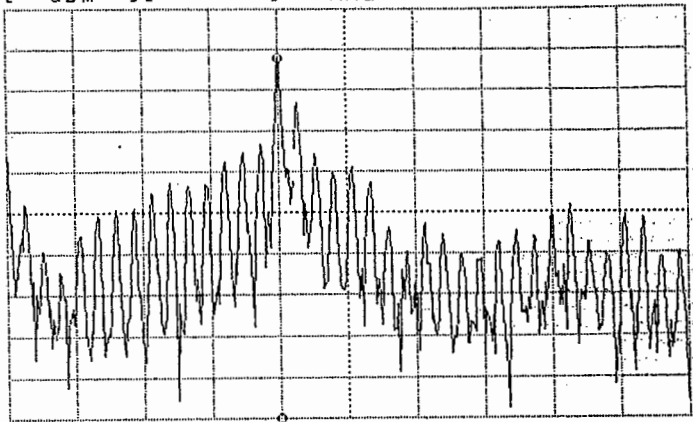
DIV 10.00 DIV 5.000 START 200.000 Hz STOP 30 000.000 Hz

PHASE RESPONSE

8 kHz



A: REF 10.00 [dBm] B: REF 0.000 [] MKR 8 000.001 Hz MAG -2.06444 dBm MAG

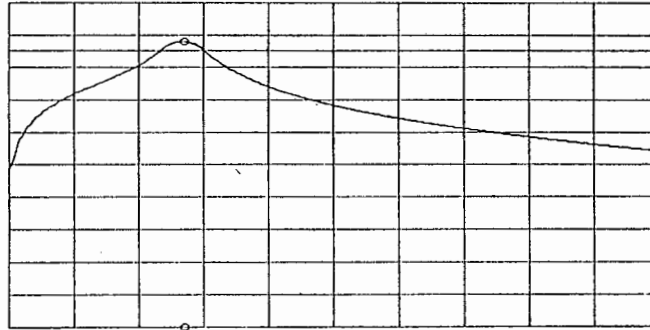


DIV 10.00 DIV 10.00 START 0.001 Hz STOP 20 000.000 Hz

Input and output spectrum

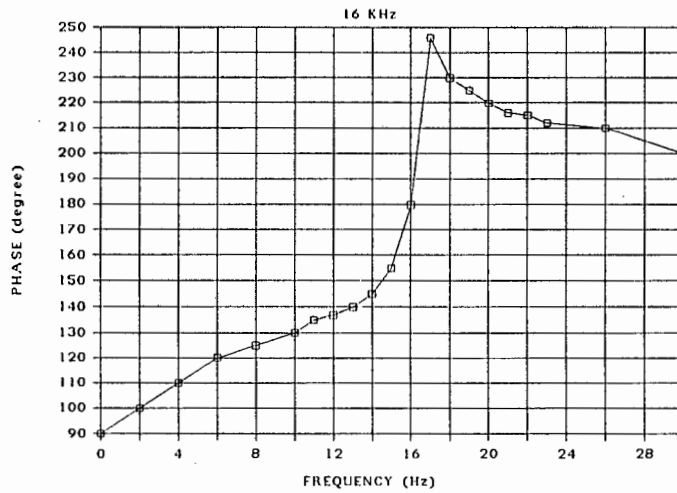
AMPLITUDE @ f = 16 kHz

A: REF B: REF ΔCRS_A -3.00000 dB
 20.00 20.00 0 3.921247217E+00
 [dBm] []

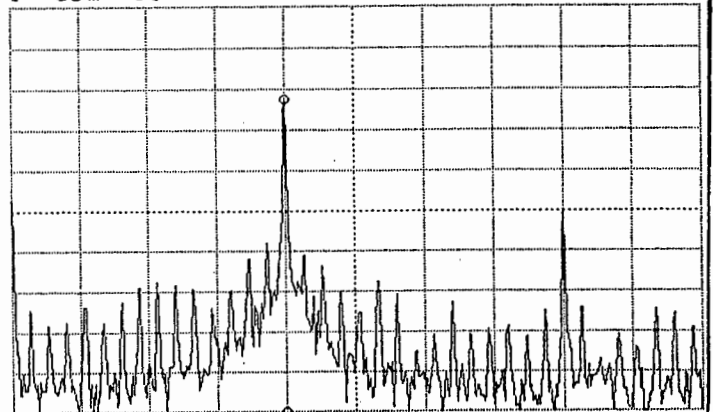
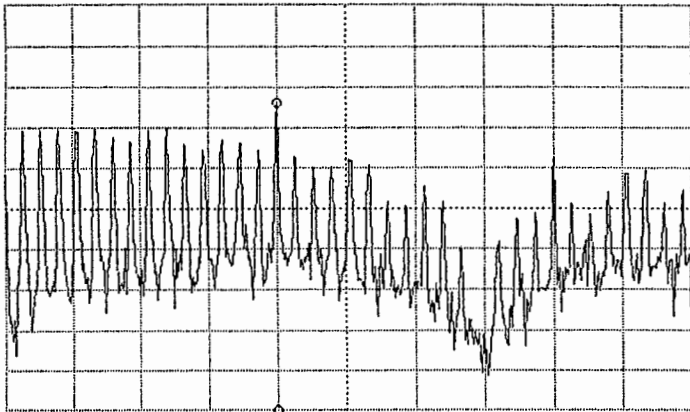


DIV DIV START 200.000 Hz
 10.00 5.000 STOP 60 000.000 Hz

PHASE RESPONSE



A: REF B: REF ○ MKR 16 000.001 Hz A: REF B: REF ○ MKR 16 000.001 Hz
 30.00 0.000 MAG 6.09674 dBm 30.00 0.000 MAG 7.68111 dBm
 [dBm] [] MAG [dBm] [] MAG



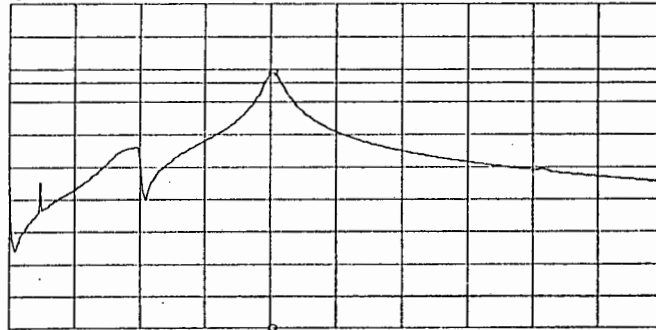
DIV DIV START 0.001 Hz
 10.00 10.00 STOP 40 000.001 Hz

DIV DIV START 0.001 Hz
 10.00 10.00 STOP 40 000.001 Hz

Input and output spectrum

AMPLITUDE @ f = 32 kHz

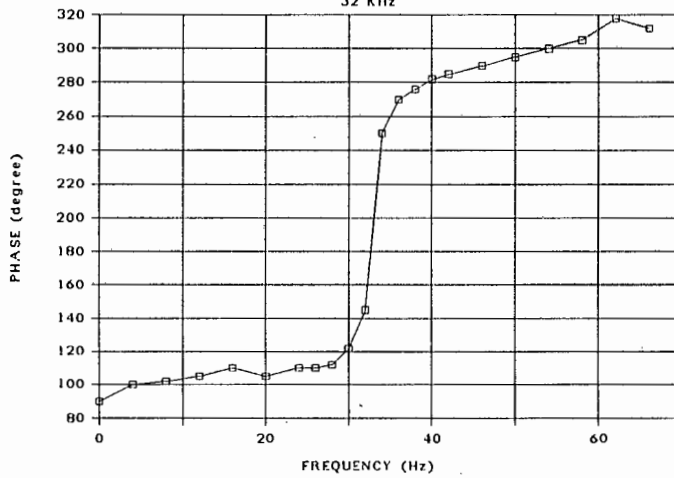
A: REF B: REF ΔCRS_A -3.00000 dB
 [20.00 dBm] [20.00] Q 1.730105294E+01



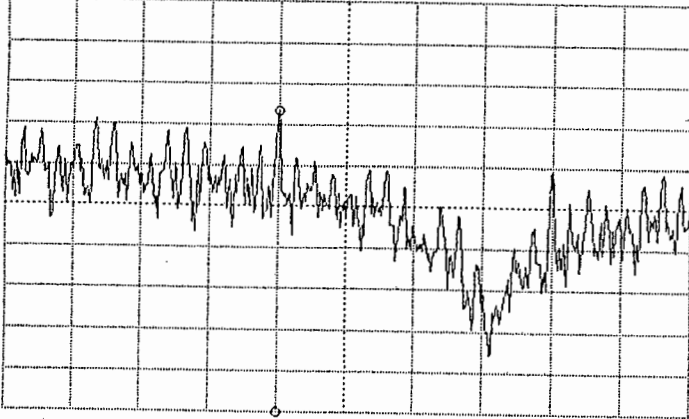
DIV 10.00 DIV 5.000 START 200.000 Hz
 STOP 80 000.000 Hz

PHASE RESPONSE

32 KHz

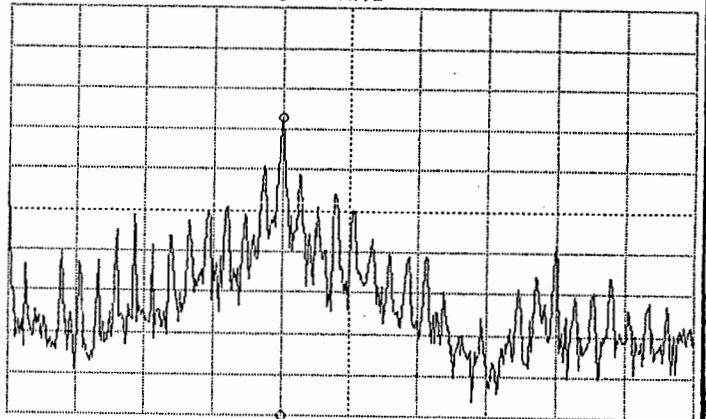


A: REF B: REF ○ MKR 32 000.001 Hz
 30.00 0.000 MAG 3.46932 dBm
 [dBm] [] MAG



DIV 10.00 DIV 10.00 START 0.001 Hz
 STOP 80 000.001 Hz

A: REF B: REF ○ MKR 32 000.001 Hz
 30.00 0.000 MAG 2.77160 dBm
 [dBm] [] MAG

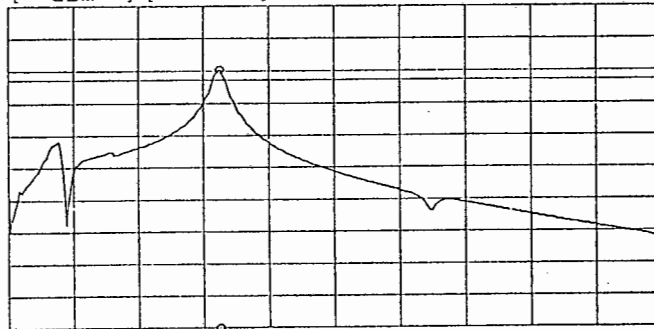


DIV 10.00 DIV 10.00 START 0.001 Hz
 STOP 80 000.001 Hz

Input and output spectrum

AMPLITUDE @ f = 64 kHz

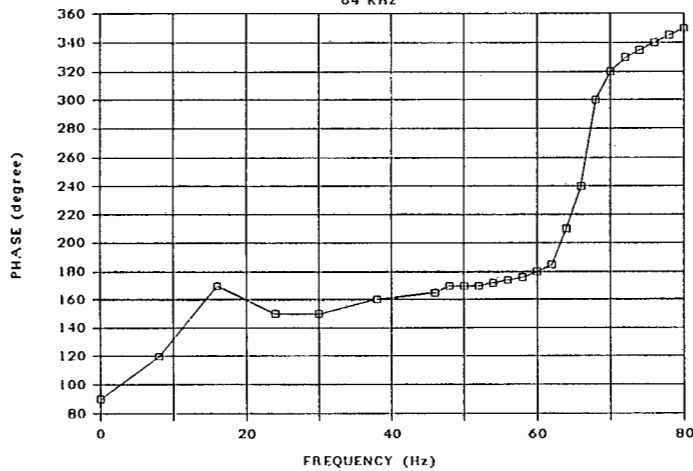
A: REF B: REF ΔCRS_A -3.00000 dB
 20.00 20.00 0 1.884585149E+01
 [dBm] []



DIV DIV START 200.000 Hz
 10.00 5.000 STOP 200 000.000 Hz

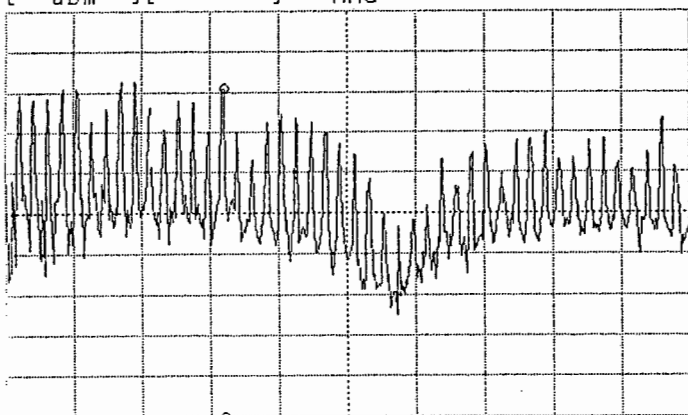
PHASE RESPONSE

64 KHz

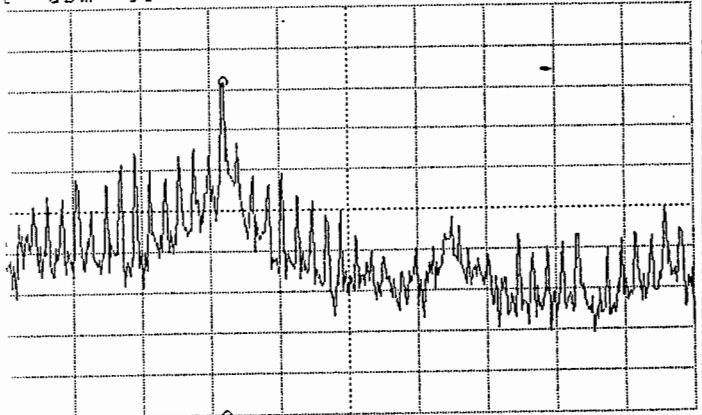


A: REF B: REF ○ MKR 64 000.001 Hz
 20.00 0.000 MAG 1.01399 dBm
 [dBm] [] MAG

A: REF B: REF ○ MKR 64 000.001 Hz
 20.00 0.000 MAG 2.18309 dBm
 [dBm] [] MAG



DIV DIV START 0.001 Hz
 10.00 10.00 STOP 200 000.000 Hz

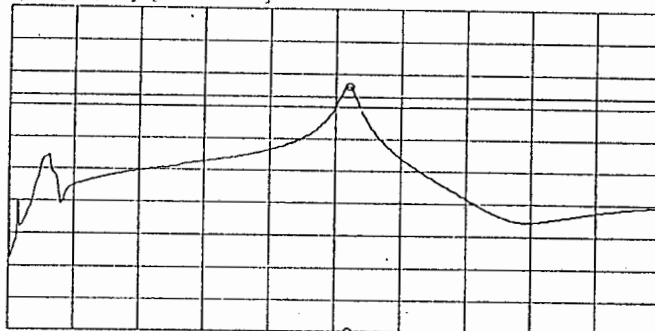


DIV DIV START 0.001 Hz
 10.00 10.00 STOP 200 000.000 Hz

Input and output spectrum

AMPLITUDE @ f = 128 kHz

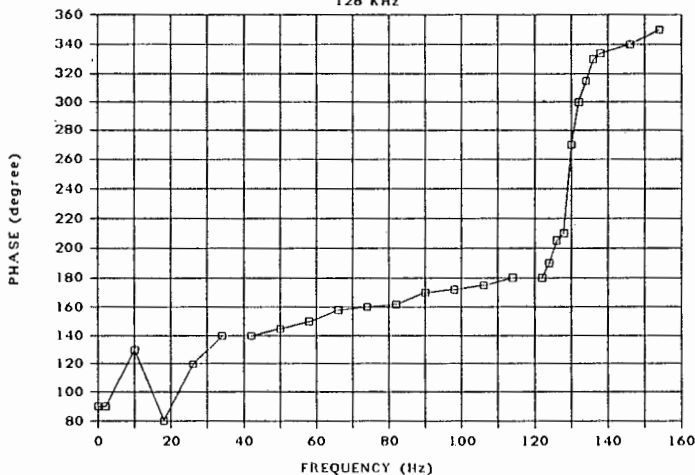
A: REF B: REF ΔCRS_A -3.00000 dB
 20.00 20.00 0 2.386286962E+01
 [dBm] []



DIV 10.00 DIV 5.000 START STOP 250 200.000 Hz
 000.000 Hz

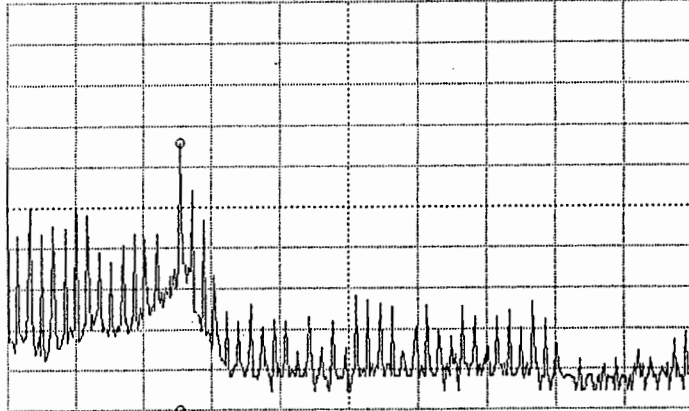
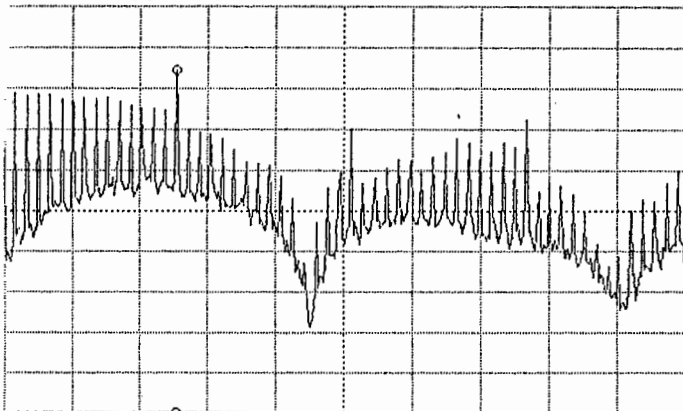
PHASE RESPONSE

128 kHz



A: REF B: REF ○ MKR 127 500.001 Hz
 20.00 0.000 .MAG 4.51825 dBm
 [dBm] [] MAG

A: REF B: REF ○ MKR 127 500.001 Hz
 20.00 0.000 MAG -14.3067 dBm
 [dBm] [] MAG



DIV 10.00 DIV 10.00 START STOP 500 0.001 Hz
 000.000 Hz

DIV 10.00 DIV 10.00 START STOP 500 0.001 Hz
 000.000 Hz

Input and output spectrum

APPENDIX F

ACTIVE BAND PASS FILTERS

1.1 CIRCUIT DIAGRAM OF SIX PARALELL BAND PASS FILTERS

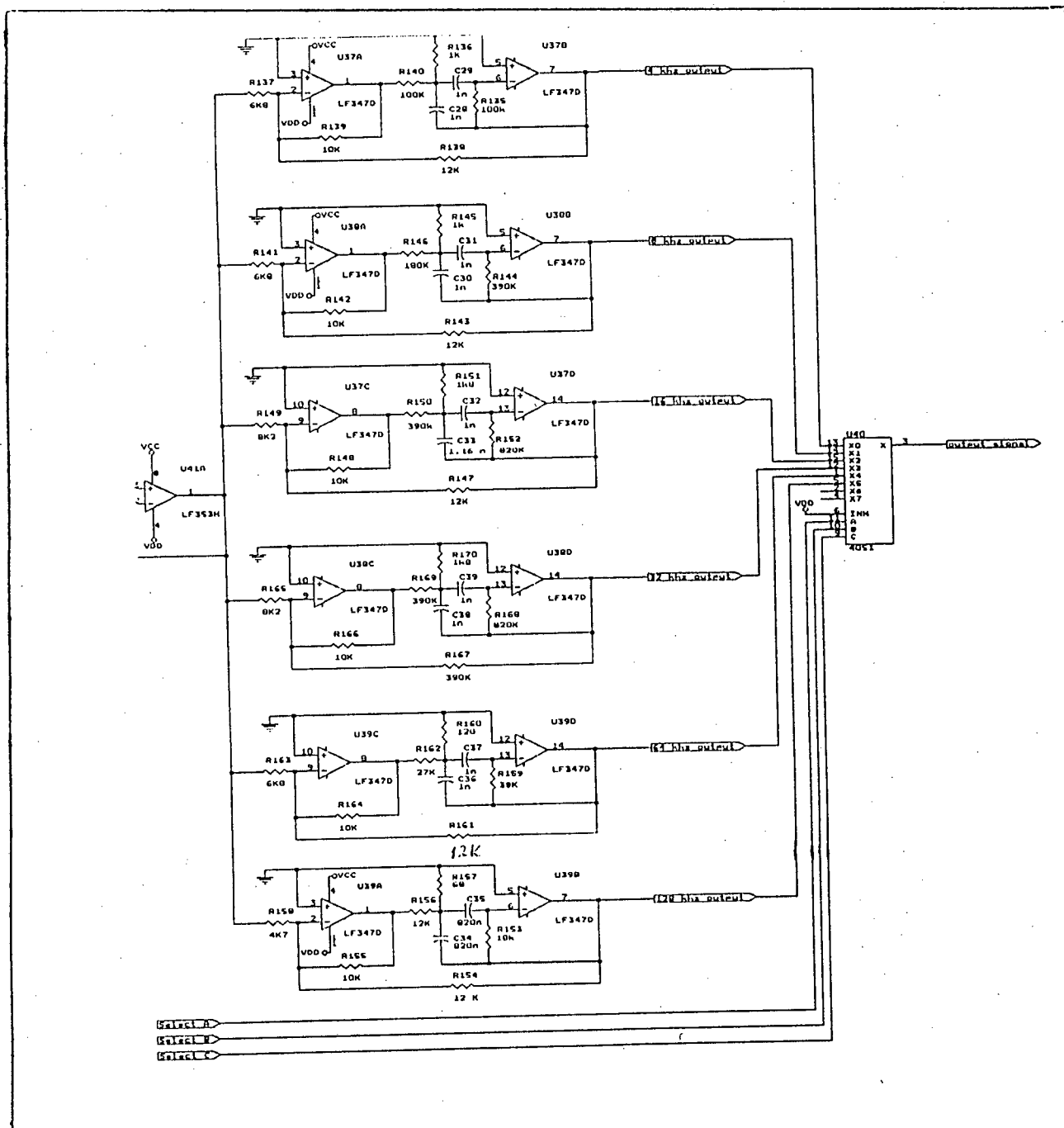


FIGURE F1 : CIRCUIT DIAGRAM OF ACTIVE BAND PASS FILTERS.

1.2 AMPLITUDE AND PHASE RESPONSE

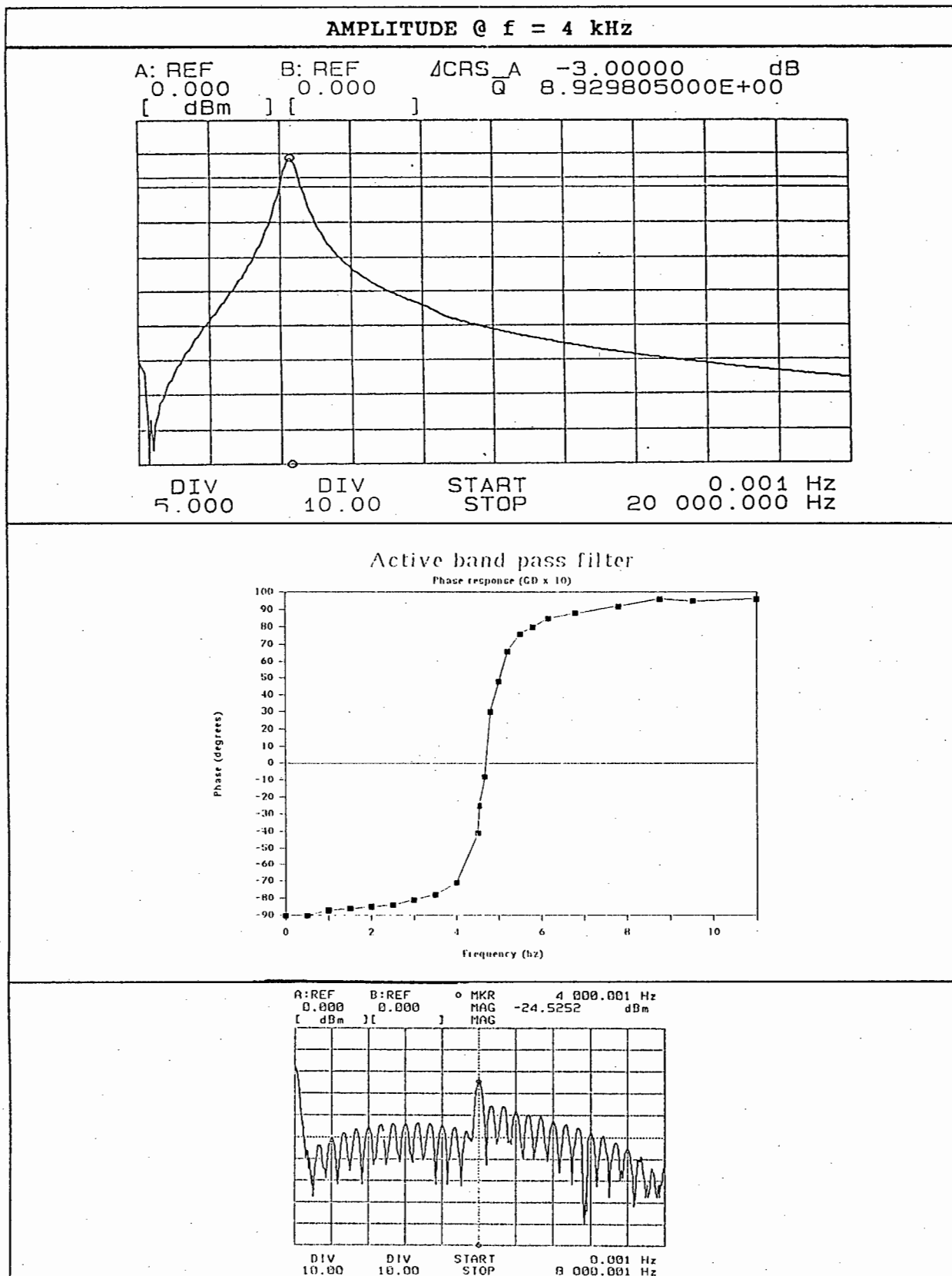
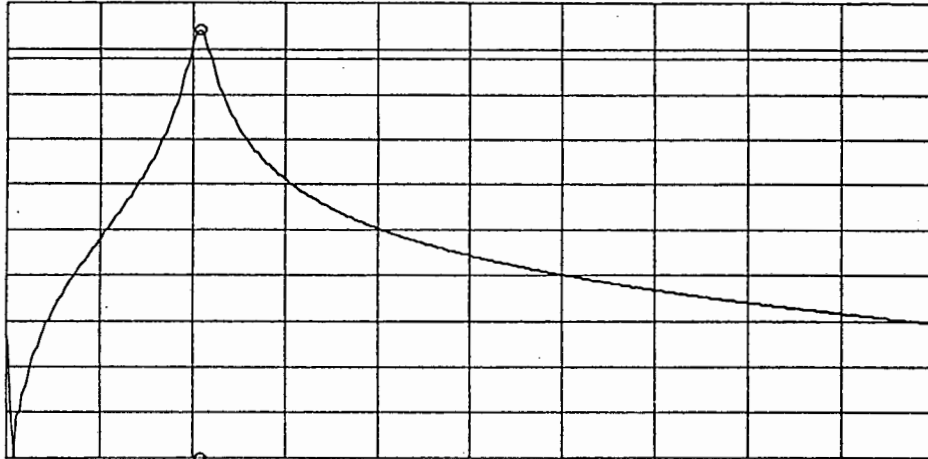


FIGURE F2 : AMPLITUDE AND PHASE RESPONSE OF FILTERS WITH OUTPUT SPECTRA.

AMPLITUDE @ f = 8 kHz

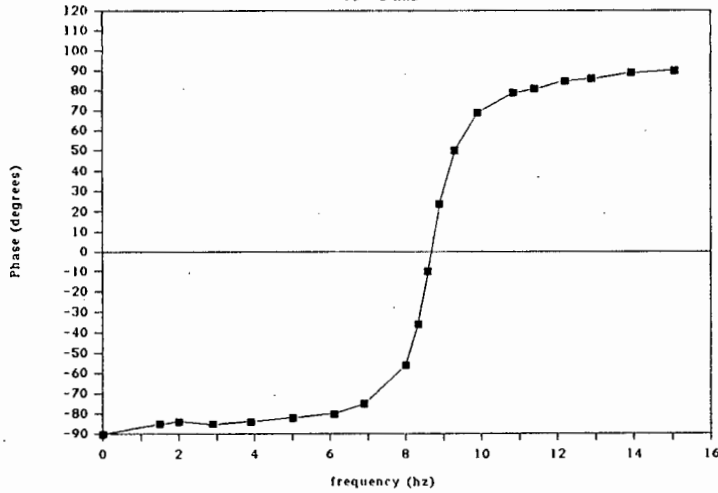
A: REF B: REF ΔCRS_A -3.00000 dB
 0.000 0.000 Q 8.836339497E+00



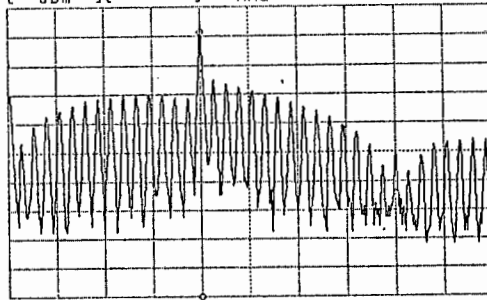
DIV DIV START 0.001 Hz
 5.000 10.00 STOP 40 000.000 Hz

Active band-pass Phase response

Fc = 8 kHz



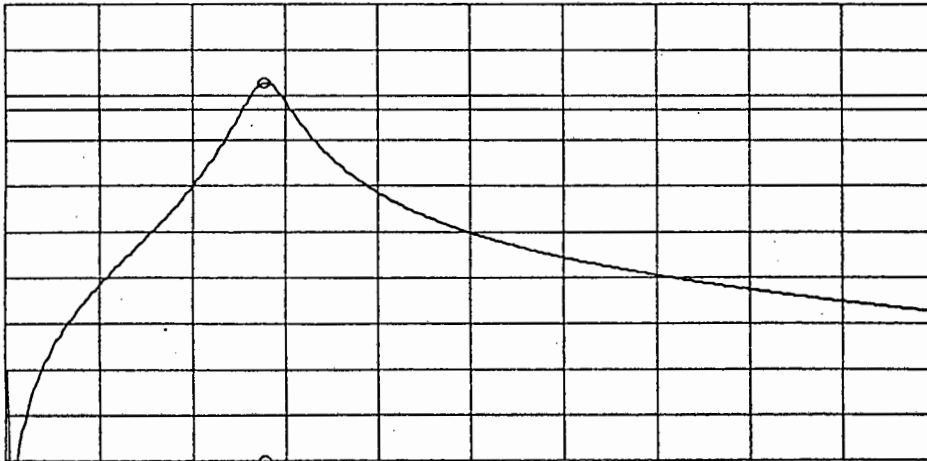
A: REF B: REF o MKR B 000.001 Hz
 -10.00 0.000 MAG -10.4999 dBm



DIV DIV START 0.001 Hz
 10.00 10.00 STOP 20 000.001 Hz

AMPLITUDE @ f = 16 kHz

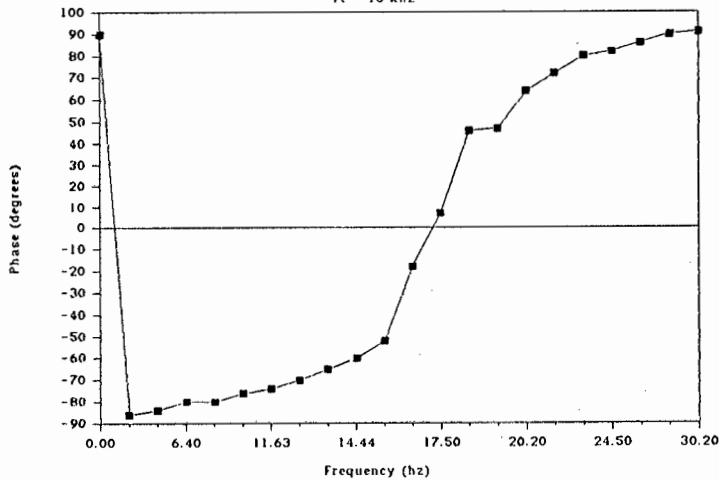
A: REF B: REF ΔCRS_A -3.00000 dB
 0.000 0.000 Q 5.339020670E+00
 [dBm] []



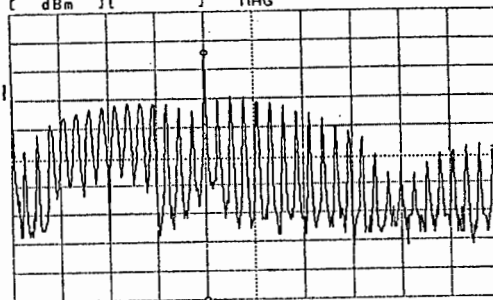
DIV DIV START 0.001 Hz
 5.000 10.00 STOP 60 000.000 Hz
 RBW: 300 Hz ST: 9.58 sec RANGE: R= 0, T= 0dBm

Active band pass filter Phase response

Fc = 16 kHz



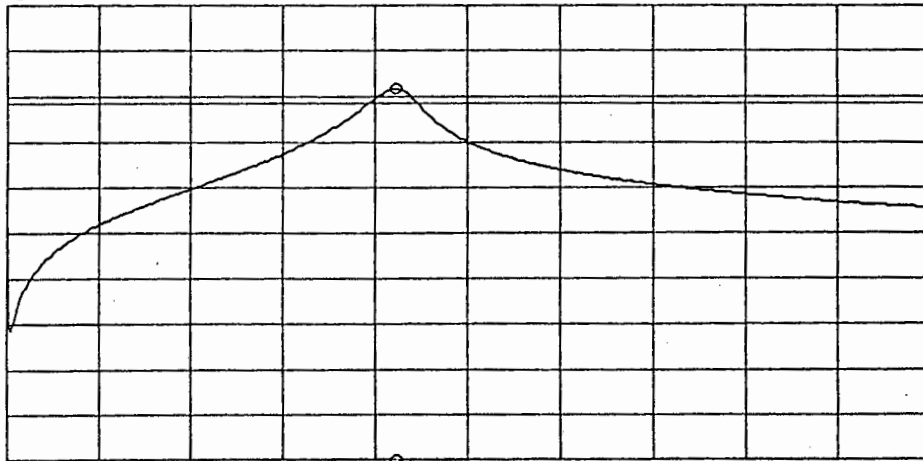
A: REF B: REF o MKR 16 000.001 Hz
 -10.00 0.000 MAG -24.3054 dBm
 [dBm] [] MAG



DIV DIV CENTER 20 000.001 Hz
 10.00 10.00 SPAN 40 000.000 Hz

AMPLITUDE @ f = 64 kHz

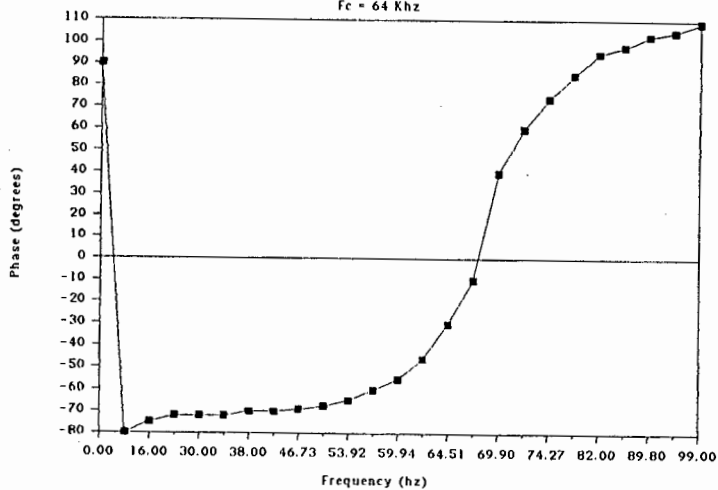
A: REF B: REF ΔCRS_A -3.00000 dB
 10.00 0.000 Q 8.089633832E+00
 [dBm] []



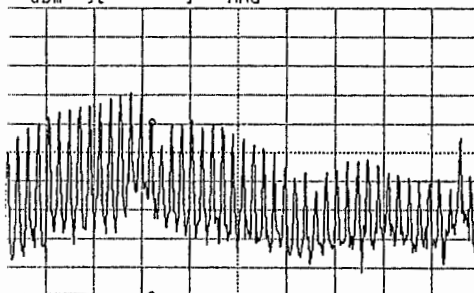
DIV 10.00 DIV 10.00 START STOP 150 100.000 Hz
 000.000 Hz

Active BPF Phase response

Fc = 64 KHz



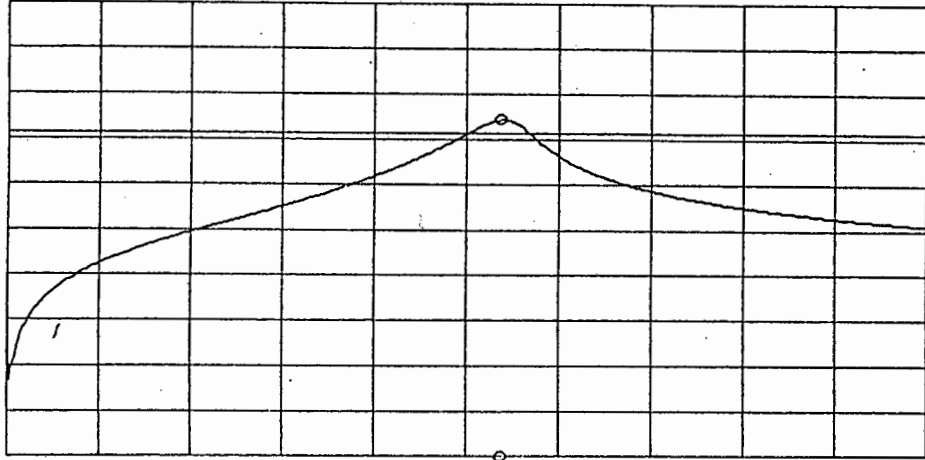
:REF B:REF o MKR 64 000.001 Hz
 10.00 0.000 MAG -49.1795 dBm
 dBm [] MAG



DIV 10.00 DIV 10.00 START STOP 0.001 Hz
 200 000.000 Hz

AMPLITUDE @ f = 128 kHz

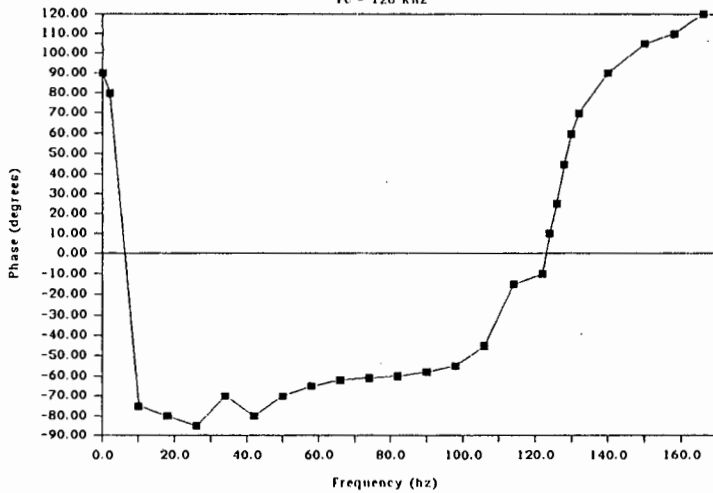
A: REF B: REF ΔCRS_A -3.00000 dB
 20.00 0.000 Q 7.971211296E+00
 [dBm] []



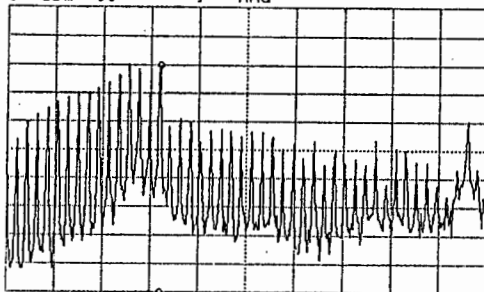
DIV DIV START 100.000 Hz
 10.00 10.00 STOP 240 000.000 Hz

Active band pass filter Phase response

Fc = 128 Khz



A: REF B: REF ○ MKR 128 000.001 Hz
 -10.00 0.000 MAG -30.0437 dBm
 [dBm] [] MAG



DIV DIV START 0.001 Hz
 10.00 10.00 STOP 400 000.000 Hz

APPENDIX G

1.1 PROBABILITY OF ERROR, $P_e = f(E_b/N_0)$

The probability of error is derived for a general receiver filter structure. The P_e vs E_b/N_0 for particular receive filters can then be derived. Two low pass receiver filters that are of interest are the ideal matched filter and the second order Butterworth filter.

The modulator performs the following mapping:

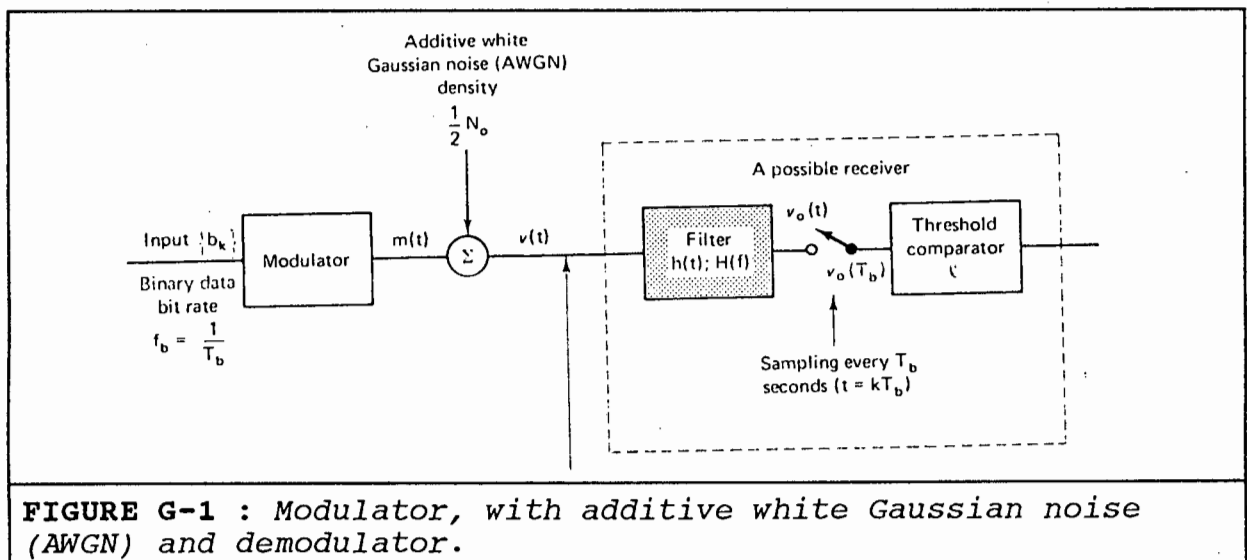
$$m(t) = \begin{cases} s_1(t) & \text{if } b_k = 0 \\ s_2(t) & \text{if } b_k = 1 \end{cases}$$

Where $s_1(t)$ and $s_2(t)$ are two elementary waveforms having a duration of T_b seconds, and having finite energy, that is,

$$E_{1b} = \int_0^{T_b} s_1^2(t) dt < \text{infinty}$$

$$E_{2b} = \int_0^{T_b} s_2^2(t) dt < \text{infinty}$$

A modulator and a possible binary demodulator are shown in Fig. G-1.



In this case, the system contains no transmit filter and only a receive filter. Therefore, 100% of the binary spectrum is transmitted.

The transfer function of the optimum receive filter, $H(f)$, its impulse response $h(t)$, and the probability of error performance of the optimum system are all obtained as a result of the following derivation.

The received carrier plus noise prior to the receive filter is

$$v(t) = \begin{cases} s_1(t) + n(t) \\ s_2(t) + n(t) \end{cases}$$

($0 < t < T_b$), depending on whether the $s_1(t)$ or $s_2(t)$ signal was transmitted. The system propagation delay is assumed to be zero. Now, let $s_1(t)$ and $s_2(t)$ be selected such that

$$s_{o1}(T_b) < s_{o2}(T_b)$$

The decision rule is based on the criteria

$$s_2(t) \text{ was sent if } v_o(T_b) > l$$

$$s_1(t) \text{ was sent if } v_o(T_b) < l$$

Where l is the threshold level of $v_o(T_b)$, the sampled output, and $s_1(t)$ and $s_2(t)$ are the signal components of the receive filter output in the sampling $t = T_b$. These filtered signals are due to the $s_1(t)$ and $s_2(t)$ transmitted signals, respectively. In the sampling instant ($t = T_b$) the signal plus noise voltage at the threshold comparator input is given by

$$v_o(T_b) = s_{o1}(T_b) + n_{o1}(T_b)$$

or

$$v_o(T_b) = s_{o2}(T_b) + n_{o2}(T_b)$$

where $n_{o1}(t)$ and $n_{o2}(t)$ represent the filtered noise components. Let the AWGN have a double-sided spectral density of

$$G_n(f) = \frac{1}{2} N_o$$

Thus the filtered noise has a power spectral density $S_{no}(f)$, given by

$$S_{no}(f) = |H(f)|^2 G_n(f)$$

$$= |H(f)|^2 \frac{1}{2} N_o$$

The receiver filter is a linear network; hence the additive Gaussian channel noise remains Gaussian after the receiver filter. The probability density function of Gaussian noise remains Gaussian even if it is filtered by a time invariant linear filter.

The noise is stationary; thus at the sampling instant, $N = n_0(T_b)$, it is a random variable with a probability density given by

$$f_N(\eta) = \frac{e^{-\frac{\eta^2}{2\sigma_o^2}}}{\sqrt{2\pi\sigma_o^2}}$$

Where the total noise power N_T (variance σ_o^2) at the receiver filter output is given by

$$N_T = \sigma_o^2 = \int_{-\infty}^{\infty} |H(f)|^2 G_n(f) df$$

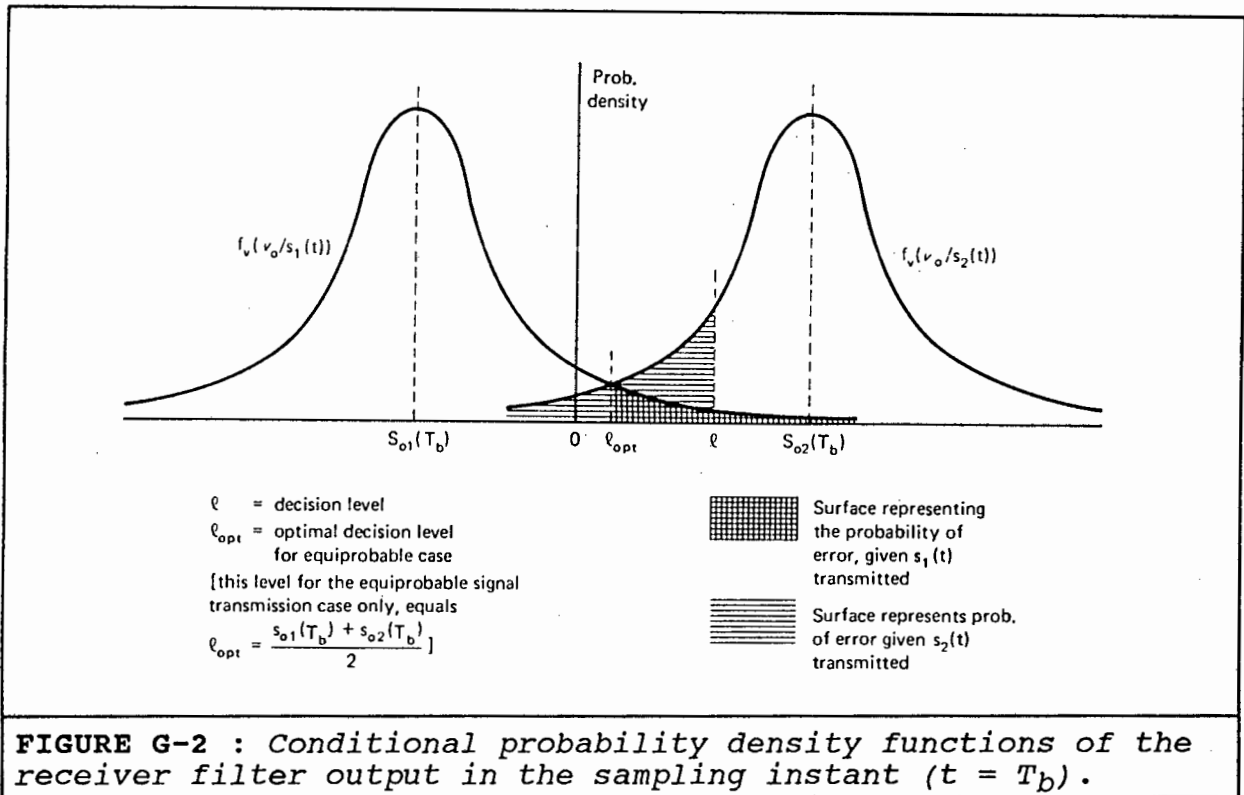
The mean value of the noise is zero, by symmetry. The sampler output has two possible states:

$$V_1 = v_1(T_b) = s_{o1}(T_b) + N \quad \text{if } s_1(t) \text{ is transmitted.}$$

or

$$V_2 = v_2(T_b) = s_{o2}(T_b) + N \quad \text{if } s_2(t) \text{ is transmitted.}$$

The conditional probability density functions (pdf) of the receive filter output in the sampling instants $t=k.T_b$ are illustrated in Fig. G-2.



The probability of error derivation.

For the general case:

Probability of transmission of an $s_1(t)$ signal is p_1 .

Probability of transmission of an $s_2(t)$ signal is p_2 .

the average probability of error is

$$P_e = p_1 \cdot P[e \setminus s_1(t)] + p_2 \cdot P[e \setminus s_2(t)]$$

It will be assumed that the transmitted signals have equal probabilities, $p_1 = p_2 = 0.5$ and

$$P_e = 0.5P(e \setminus s_1(t)) + 0.5P(e \setminus s_2(t)) \quad (G.1)$$

The probability of error, assuming that $s_1(t)$ is transmitted, is given by

$$P[e \setminus s_1(t)] = \int_l^\infty f_{v_o}[v_o \setminus s_1(t)] dv$$

$$= \int_l^{\infty} \frac{e^{-\frac{[v_o - s_{o1}(T)]^2}{2\sigma_o^2}}}{\sqrt{2\pi\sigma_o^2}} dv_o \quad (G.2)$$

Similarly for $s_2(t)$.

These probabilities are shown as shaded surfaces in Fig. G-2. Combining equations (G.1) and (G.2),

$$P_o = \frac{1}{2} \int_l^{\infty} \frac{1}{\sqrt{2\pi N_T}} e^{-\frac{[v_o - s_{o1}]^2}{2N_T}} dv_o + \frac{1}{2} \int_{-\infty}^l \frac{1}{\sqrt{2\pi N_T}} e^{-\frac{[v_o - s_{o2}]^2}{2N_T}} dv_o \quad (G.3)$$

The optimum threshold level l_{opt} can be derived by finding the first differential with respect to l in expression (G.3). If the first differential is set to zero, the optimum setting of the threshold level l is obtained:

$$l_{opt} = 0.5[s_{o1}(T_b) + s_{o2}(t_b)]$$

This level is at the intersection of the two conditional pdf's illustrated in Fig. G-2.

Insertion of the best choice of the threshold level l_{opt} into equation (G.3) gives:

$$P_o = 0.5 \operatorname{erfc} \left[\frac{s_{o2}(T_b) - s_{o1}(T_b)}{2\sqrt{2}\sigma_o} \right] \quad (G.4)$$

Where $\operatorname{erfc}(y)$ is defined by

$$\operatorname{erfc}(y) \Leftrightarrow \frac{2}{\sqrt{\pi}} \int_y^{\infty} e^{-z^2} dz \quad y > 0$$

This integral is given by tables [3.1].

1.2 TRANSFER FUNCTION OF THE OPTIMAL RECEIVER

From equation (G.4) it can be concluded that the probability of error is a function of the difference (distance) between the two output signals in the sampling instant, $t = T$, and of the rms noise voltage σ_o . The optimum filter transfer function $H(f)$, that leads to the smallest P_e , and therefore best performance, is obtained by maximisation of the ratio

$$y = \frac{s_{o2}(T_b) - s_{o1}(T_b)}{\sigma_o} \quad (G.5)$$

The derivation is simplified by maximising y^2 , eliminating the requirement $s_{o1}(T_b) < s_{o2}(T_b)$

Let the difference in the filtered outputs be

$$S_{od}(t) = S_{o2}(t) - S_{o1}(t)$$

and the difference in the sampling instants by

$$S_{od}(t) = S_{o2}(T_b) - S_{o1}(T_b)$$

Thus

$$y^2 = \frac{s_{od}^2(T_b)}{\sigma_o^2} = \frac{s_{od}^2(T_b)}{E\{n_o^2(T_b)\}} \quad (G.6)$$

The difference of the filtered outputs may be obtained by inverse Fourier transform,

$$s_{od}(t) = F^{-1}[S_{od}(f)H(f)] = \int_{-\infty}^{\infty} H(f)S_{od}(f)e^{j2\pi ft} df \quad (G.7)$$

The noise power (variance) of the stationery noise process at the filter output is given by

$$\begin{aligned} \sigma_o^2 &= E\{n_o^2(T_b)\} \\ &= \int_{-\infty}^{\infty} G_n(f)|H(f)|^2 df \\ &= \frac{1}{2}N_o \int_{-\infty}^{\infty} |H(f)|^2 df \quad (G.8) \end{aligned}$$

Combining equations (G.7) and (G.8) and substituting into (G.6), we obtain

$$y^2 = \frac{\left| \int_{-\infty}^{\infty} H(f)S_{od}(f)e^{j2\pi fT_b} df \right|^2}{\frac{1}{2}N_o \int_{-\infty}^{\infty} |H(f)|^2 df}$$

To maximise y^2 we employ *Schwartz's inequality*. This inequality states

$$\left| \int_{-\infty}^{\infty} X(f)Y(f)^* df \right|^2 \leq \int_{-\infty}^{\infty} |X(f)|^2 df \int_{-\infty}^{\infty} |Y(f)|^2 df$$

where $X(f)$ and $Y(f)$ are arbitrary complex functions of a common variable f . Equality holds if

$$X(f) = kY^*(f)$$

where k is an arbitrary constant and $Y^*(f)$ is the complex conjugate of $Y(f)$. The following substitution can be done to The Schwartz inequality, put

$$X(f) = H(f)$$

$$Y^*(f) = S_{od}(f)e^{j2\pi f T_b}$$

This results in

$$\gamma^2 = \frac{1}{G_n(f)} \frac{\left| \int_{-\infty}^{\infty} X(f)Y^*(f)df \right|^2}{\int_{-\infty}^{\infty} |H(f)|^2 df}$$

Applying Schwartz's inequality

$$\leq \frac{2}{N_o} \int_{-\infty}^{\infty} |H(f)|^2 df \frac{\int_{-\infty}^{\infty} |S_{od}(f)|^2 df}{\int_{-\infty}^{\infty} |H(f)|^2 df}$$

$$\Rightarrow \gamma^2 \leq \frac{2}{N_o} \int_{-\infty}^{\infty} |S_{od}(f)|^2 df \quad (G.9)$$

Based on Schwartz's inequality and the additive white Gaussian noise assumption, $G_n(f) = N_o/2$, it can be concluded that the equality holds, i.e. the signal-to noise ratio is maximised if

$$H(f) = m S_{od}^*(f) e^{-j2\pi f T_b}$$

where m is a constant that represents the receiver filter gain. The gain constant of linear filters has evidently no influence on the output signal-to-noise ratio. Thus, without loss of generality, set $m = 1$. The optimum receiver transfer function $H_o(f)$ is thus given by

$$H_o(f) = S_{od}^*(f) e^{-j2\pi f T_b} \quad (G.10)$$

APPENDIX H

THE COMPLETE CIRCUIT DIAGRAM

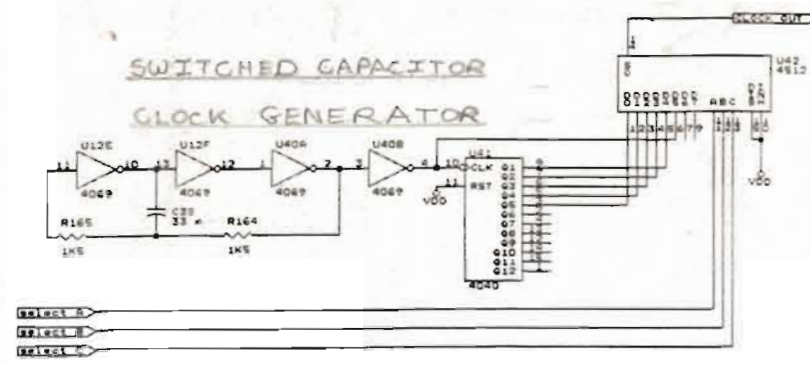
of the

MODULATOR AND DEMODULATOR

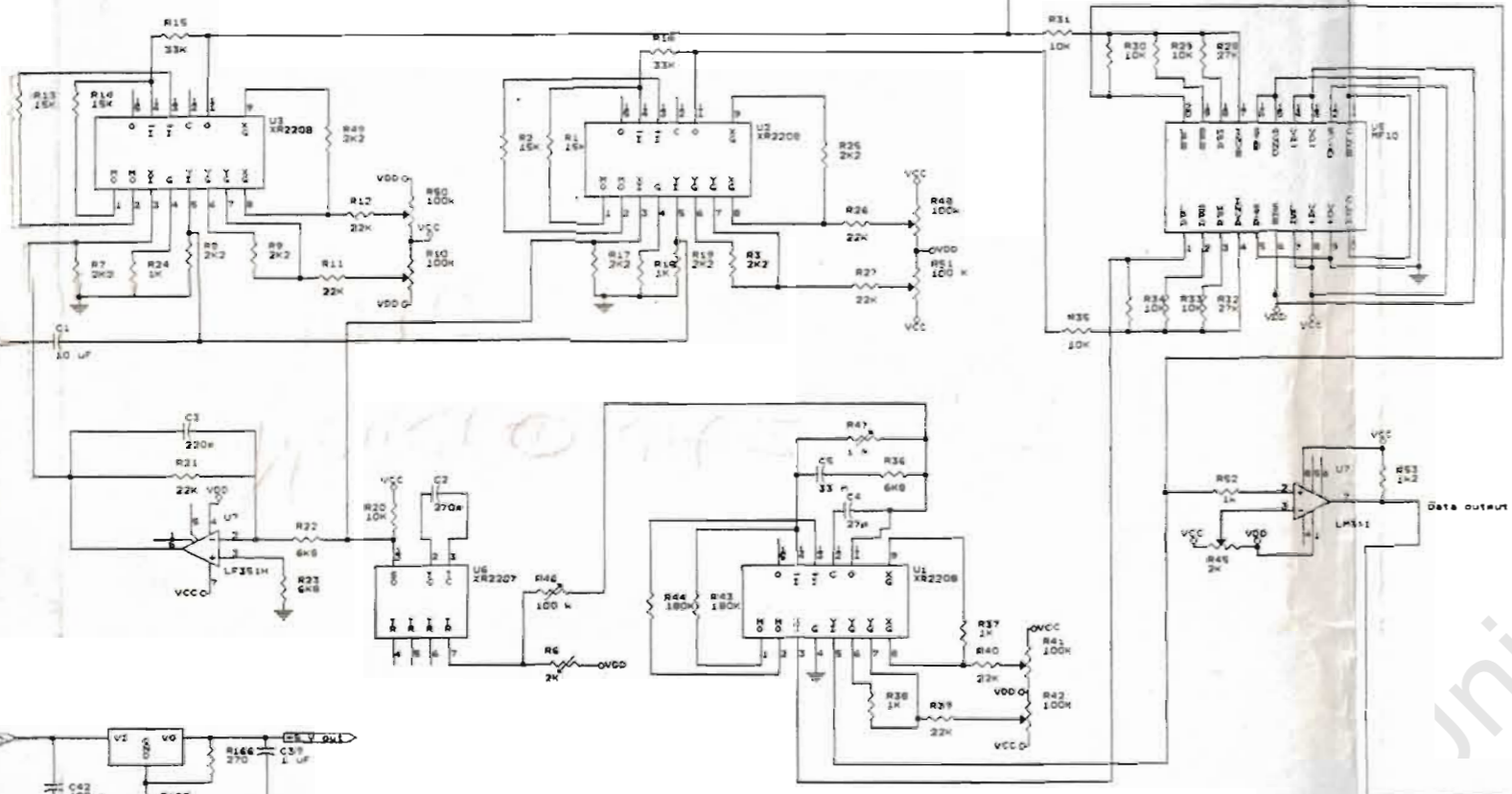
MODULATOR

DEMODULATOR

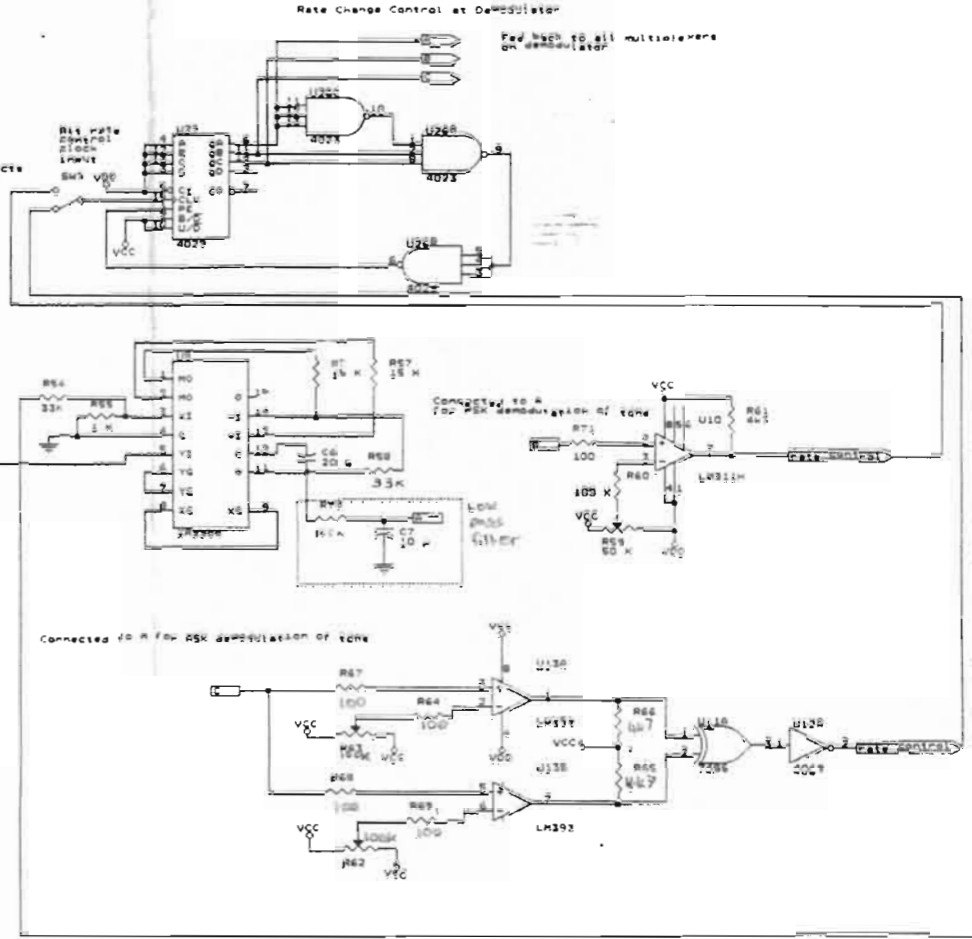
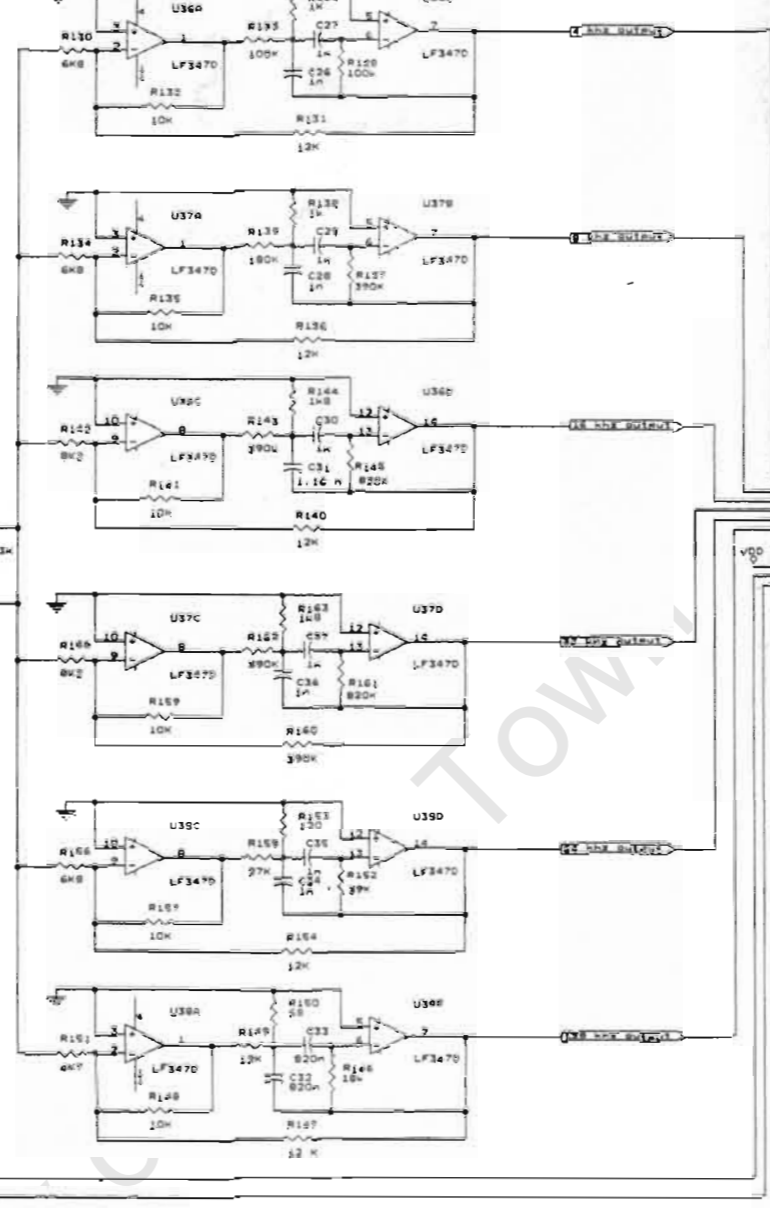
**SWITCHED CAPACITOR
CLOCK GENERATOR**



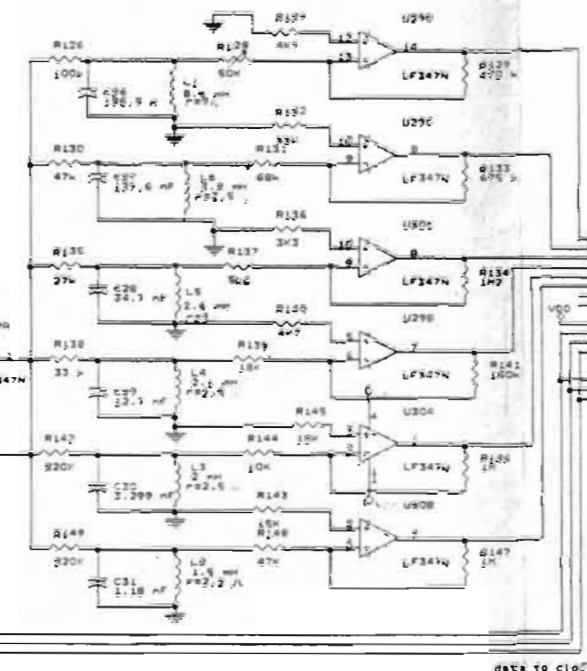
COSTAS LOOP



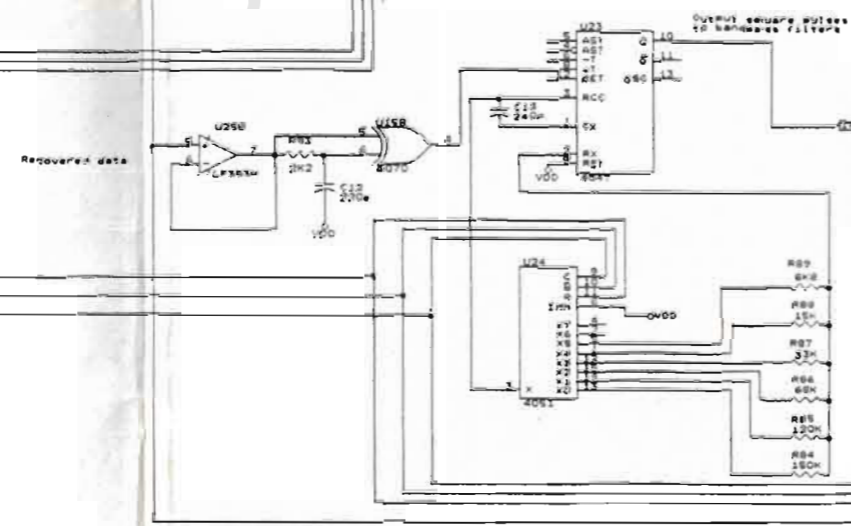
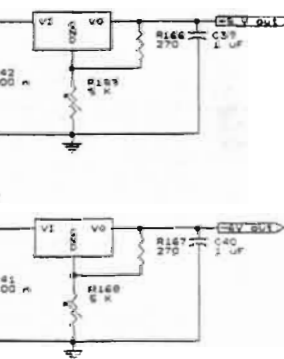
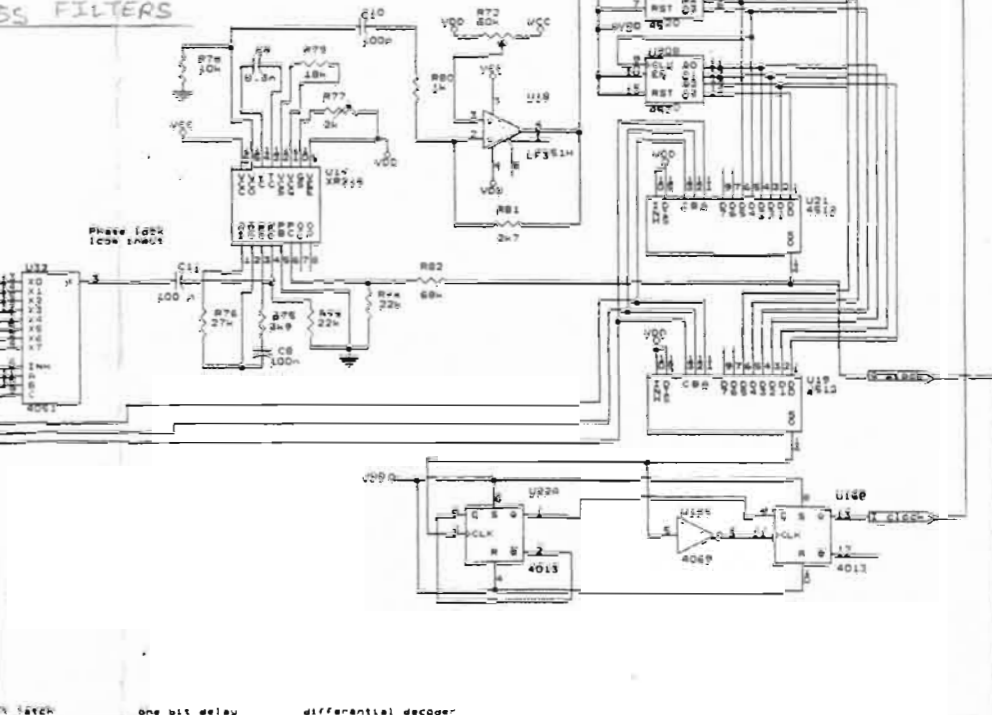
**BANK OF SIX ACTIVE BAND
PASS FILTERS**



BANK OF SIX PASSIVE BAND PASS FILTERS



PHASE LOCK LOOP



NOTE:
- For all power points
- VDD = +5V
- VCC = +12V
- GND = 0V chassis connection

